Hepatic inflammation facilitates transcription-associated mutagenesis via AID activity and enhances liver tumorigenesis

Tomonori Matsumoto, Takahiro Shimizu, Norihiro Nishijima, Atsuyuki Ikeda, Yuji Eso, Yuko Matsumoto, Tsutomu Chiba, and Hiroyuki Marusawa*

Department of Gastroenterology and Hepatology,
Graduate School of Medicine, Kyoto University, Kyoto 606-8507, Japan.

***Corresponding & Reprint Author:** Hiroyuki Marusawa, M.D., Ph.D.
Department of Gastroenterology and Hepatology,
Graduate School of Medicine, Kyoto University,
54 Kawara-cho, Shogoin, Sakyo-ku, Kyoto 606-8507, Japan
Phone; +81-75-751-4302
Fax; +81-75-751-4303
E-mail; maru@kuhp.kyoto-u.ac.jp

Running title: Inflammation-enhanced mutagenesis and liver cancer

Key words: AID, hepatitis, liver cancer, single nucleotide variant

Abstract

Chronic inflammation triggers the aberrant expression of a DNA mutator enzyme, activation-induced cytidine deaminase (AID), and contributes to tumorigenesis through the accumulation of genetic aberrations. To gain further insight into the inflammation-mediated genotoxic events required for carcinogenesis, we examined the role of chronic inflammation in the emergence of genetic aberrations in the liver with constitutive AID expression. Treatment

with thioacetamide (TAA) at low-dose concentrations caused minimal hepatic inflammation in both wild-type and AID transgenic (Tg) mice. None of the wild-type mice with low-dose TAA administration or AID Tg mice without hepatic inflammation developed cancers in their liver tissues over the 6-month study period. In contrast, all the AID Tg mice with TAA treatment developed multiple macroscopic hepatocellular carcinomas during the same observation period. Whole exome sequencing and additional deep-sequencing analyses revealed the enhanced accumulation of somatic mutations in various genes, including *dual specificity phosphatase 6* (*Dusp6*), *early growth response 1* (*Egr1*) and *inhibitor of DNA binding 2* (*Id2*), which are putative tumor suppressors, in AID-expressing liver with TAA-mediated hepatic inflammation. Microarray and quantitative reverse transcription-polymerase chain reaction analyses showed the transcriptional upregulation of various genes including *Dusp6*, *Egr1* and *Id2* under hepatic inflammatory conditions. Together, these findings suggest that inflammation-mediated transcriptional upregulation of target genes, including putative tumor suppressor genes, enhances the opportunity for inflamed cells to acquire somatic mutations and contributes to the acceleration of tumorigenesis in the inflamed liver tissues.

Summary

Chronic inflammation triggers expression of a mutator enzyme, activation-induced cytidine deaminase (AID), and induces tumorigenesis through mutation accumulation. We demonstrated that hepatic inflammation under constitutive AID expression accelerated hepatocarcinogenesis by accumulating mutations especially in transcriptionally upregulated genes including tumor suppressors.

Introduction

Chronic inflammation plays a critical role in tumor development. Indeed, various human cancers develop in the background of inflamed epithelial organs. A variety of molecular mechanisms underlying inflammation-associated tumorigenesis have been proposed, including inflammation-mediated dysregulation of cellular homeostasis (1–3). Inflammation triggers the acceleration of cell proliferation by activating transcription factors such as nuclear factor-kappa B (NF-κB) and signal transducer and activator of transcription 3 (STAT3) in premalignant cells via the stimulation of proinflammatory cytokines (2). Anti-apoptotic phenotypes are also evoked by activation of NF-κB (2). Moreover, infiltrating cells, including tumor-associated macrophages, enhance tumorigenesis by producing growth factors and angiogenic factors (2). These biologic responses induced by inflammation could predispose to tumorigenesis in a coordinated manner. They should, however, eventually merge into genetic or epigenetic changes, and the accumulation of genetic alterations in tumor-related genes is a critical step required for malignant transformation (1,3).

Accumulating evidence indicates that somatic mutations in tumor-related genes could be detectable in inflamed epithelial cells before tumor onset. Several studies revealed the accumulation of genetic alterations of tumor-related genes in background nontumorous tissues with underlying inflammatory conditions (4,5). We recently reported latent accumulation of a large number of somatic mutations in hepatitis C virus-infected nontumorous cirrhotic liver tissues, which is at extremely high risk for hepatocarcinogenesis (6). Similarly, chronic gastritis tissues infected with *Helicobacter pylori* accumulate genetic aberrations prior to the detection of gastric cancer (7). These findings indicate that chronic inflammation leads to somatic mutations in inflamed epithelial cells and that those cells with accumulated alterations in tumor-related genes acquire the potential for malignant transformation. How these cells acquire genetic aberrations under inflammatory conditions, however, remains to be elucidated.

The discovery of intrinsic DNA mutator enzymes opened doors to studying the molecular link between inflammation and genetic alterations during tumor development. The apolipoprotein B mRNA-editing enzyme catalytic polypeptide (APOBEC) family comprises nucleotide editing enzymes that induce nucleotide alterations in target DNA or RNA through their cytidine deamination activity (8). Among them, activation-induced cytidine deaminase (AID) is well characterized by its ability to induce nucleotide alterations and double-strand DNA breaks in human DNA sequences (9,10). Under physiologic conditions, the mutagenic activity of AID contributes to generating antibody gene diversification in activated B lymphocytes by inducing somatic hypermutation and class-switch recombination of immunoglobulin genes (9,11). Aberrantly expressed AID in epithelial cells, however, could induce mutations in various nonimmunoglobulin genes and may be involved in inflammation-associated tumorigenesis in gastrointestinal organs (12–16). To gain further insight into the role of inflammation in the emergence of somatic mutations during tumor development, we examined whether constitutive inflammation enhances the susceptibility to mutagenesis and resultant tumorigenesis. Here we demonstrated that chronic hepatic inflammation mediated by the administration of low-dose thioacetamide (TAA) substantially accelerated the development of liver tumors through an enhanced accumulation of somatic mutations mediated by the cytidine deamination activity of AID. Our findings provide a putative link between transcriptional upregulation of various cancer-related genes under inflammatory conditions and the enhanced opportunity for inflamed cells to acquire the somatic mutations required for tumorigenesis.

Materials and methods

Animal experiments

AID transgenic (Tg) mice on the C57BL/6 background were described previously (17). Thioacetamide (Sigma, St. Louis, MO, USA) was diluted in drinking water to produce a 0.01%, 0.02% or 0.03% (w/v) solution, and administered to wild-type (WT) C57BL/6 mice and AID Tg mice for 6 months continuously. Liver tissue samples were collected after TAA administration, and then some of them were fixed in 10% buffered formalin for histologic analyses, and some were frozen for analyses of genomic mutation and mRNA expression. Serum alanine aminotransferase (ALT) levels were measured with the enzymatic assay kit (Wako, Osaka, Japan). All animal experiments were approved by the ethics committee for animal experiments and performed according to the Guidelines for Animal experiments of Kyoto University.

Histologic and immunofluorescence analyses

For histologic analyses, the fixed liver tissues were embedded in paraffin, sectioned at 5 μm and stained with hematoxylin-eosin and Masson's trichrome stain. For immunofluorescence staining, the fixed liver tissues were embedded in optimum cutting temperature compound (Sakura Finetechnical, Tokyo, Japan), frozen in liquid nitrogen, and sectioned at 7 μm. Immunofluorescence staining was performed using rabbit anti-Ki67 (1:1000, Novocastra, Newcastle, UK) and rat anti-E-cadherin (1:100, Takara, Tokyo, Japan) as primary antibodies, and Alexa Fluor 488 goat anti-rabbit IgG (1:200; Thermo Fisher Scientific, Waltham, MA, USA) and Dylight 549 donkey anti-rat IgG (1:200; Jackson ImmunoResearch, West Grove, PA, USA) as secondary antibodies. Nuclei were visualized with DAPI (Vector Laboratories H-1200, Burlingame, CA, USA).

Semiquantitative and quantitative reverse transcription-polymerase chain reaction (RT-PCR) and microarray analyses

Total RNA was isolated with RNeasy Mini Kit (Qiagen, Valencia, CA) or the Sepasol RNA-I (Nacalai Tesque, Kyoto, Japan), and cDNA was synthesized using a Transcriptor High Fidelity cDNA Synthesis Kit (Roche, Basel, Switzerland). PCR amplification was performed using Takara Ex Taq DNA polymerase (Takara) with the oligonucleotide primers described previously (18). Quantitative real-time PCR was performed using LightCycler 480 System II (Roche) and the oligonucleotide primers used are shown in Supplementary Table 1. To assess the quantity of isolated RNA and the efficiency of cDNA synthesis, target cDNAs were normalized to the expression levels of an endogenous housekeeping reference gene, 18S rRNA (19). For simplicity, the expression levels of the target gene are expressed as relative values compared with the WT control. Microarray analysis was performed using Mouse GE 4x44k v2 microarrays (Agilent Technologies, Santa Clara, CA, USA) as previously described (20,21). Microarray data were deposited in the GEO database; accession number GSE62878.

Whole exome capture and massively-parallel sequencing

WT and AID Tg mice analyzed by whole exome sequencing in the present study were littermates from the same cross. Genomic DNA was extracted from the liver tissues using a DNeasy Blood & Tissue Kit (Qiagen). Massively-parallel sequencing was performed using the Illumina Genome Analyzer IIx (Illumina, San Diego, CA, USA) as previously described (7,22,23). Briefly, the DNA libraries were prepared from fragmented DNA (>5 μg) with an Illumina Preparation Kit (Illumina). Whole exome sequence capture was then performed using SeqCap EZ Developer Library (Roche). Cluster generation and paired-end sequencing for 2 × 76 base pair reads were performed as previously described (7). Sequencing data were deposited in the DNA Data Bank of Japan Sequence Read Archive; accession number DRA003477.

Whole exome sequencing analysis and variant filtering

Sequencing data were analyzed with high performance alignment software, NextGENe 2nd Generation Sequence Analysis Software v2.2.0 (SoftGenetics, State College, PA, USA). The 76 base-pair reads obtained from the Genome Analyzer IIx were aligned with the reference sequences of *Mus musculus* whole genome derived from the NCBI build 37.1 annotation, and candidate somatic mutations were selected according to the variant filtering process as previously described with modification (20). As shown in Supplementary Figure 1, to exclude common variants in mice, single nucleotide variations present in the liver of WT C57BL/6 mouse at a frequency of greater than 5% were filtered out. Furthermore, to minimize the number of false positives, the remaining single nucleotide variations were subsequently filtered according to the following criteria: (a) the coverage must be ≥15; (b) a predicted mutant allele must be present in at least 15% of the total reads; and (c) at least 4 mutant alleles were detected.

Deep sequencing analysis on selected genes

Mutational status of *Dusp6*, *Egr1* and *Id2* genes was investigated by high-coverage sequencing analyses. Target regions were designed within the range from 150 to 170 bp, and the primer sequences for target amplification are shown in Supplementary Table 2. Each region was amplified by PCR using Phusion High-Fidelity DNA Polymerase (Thermo Fisher Scientific) and purified by gel-extraction methods. Each sample was dA-tailed and ligated to adaptors containing tag sequences, followed by emulsion PCR and sequencing using the GS Junior System (Roche), as previously described (7). Deep sequencing data were analyzed with NextGENe software, and somatic mutations were identified by the variant filtering process shown in Supplementary Figure 2.

Subcloning and Sanger sequencing analyses

Oligonucleotide primers for amplification of the murine *Id2*, *Dusp6* and *Egr1* genes are shown in Supplementary Table 3. Amplification of the targeted sequences was performed using

Phusion High-Fidelity DNA Polymerase, and the products were subcloned into a pcDNA3 vector (Thermo Fisher Scientific). The resulting plasmids were sequenced using BigDye Terminator v3.1 Cycle Sequencing Kit (Thermo Fisher Scientific) on Applied Biosystems 3500 Genetic Analyzer (Thermo Fisher Scientific).

Statistical analysis

Statistical analysis was performed using the Mann–Whitney *U* test and unpaired t test. Differences were considered to be statistically significant if *P*-values were <0.05.

Results

Administration of low-dose TAA induced chronic hepatic inflammation

To induce chronic hepatic inflammation, we administered TAA at various concentrations in the drinking water to WT mice. Consistent with a previous study (24), TAA treatment at a conventional concentration (0.03%) induced hepatic inflammation with elevated levels (>45 IU/l) of ALT, whereas lower-dose TAA administration at a concentration of either 0.01% or 0.02% elicited only a slight increase in ALT throughout the 6-month administration period (Figure 1A). Histologic analysis revealed that WT mice treated with low-dose TAA for 8 weeks exhibited minimal inflammatory findings with small numbers of mononuclear cells mainly infiltrating the periportal area (Figure 1B). Semiquantitative RT-PCR analyses revealed that the expression levels of proinflammatory cytokines, such as interleukin-6, interleukin-1β and tumor necrosis factor-α (TNF-α), were elevated in the liver tissues of WT mice treated with low-dose TAA (Figure 1C). Immunohistochemistry revealed the expansion of cells positive for E-cadherin and Ki-67 in TAA-treated liver tissues (Figure 1D), suggesting active proliferation of hepatocytes in response to liver inflammation. These findings indicated that administration of low-dose TAA causes chronic minimal inflammation in liver tissues in association with enhanced proliferation of hepatocytes.

Constitutive AID expression concurrent with hepatic inflammation markedly facilitated liver tumorigenesis

We previously demonstrated that AID Tg mice with constitutive and ubiquitous AID expression developed hepatocellular carcinoma (HCC) through the accumulation of somatic mutations in their liver tissues, although it usually takes over a year for the mice to acquire the genetic aberrations required for tumorigenesis (25). Consistent with this finding, we confirmed that none of the 6-month-old AID Tg mice examined developed any tumors in their liver tissues

(Table 1). Then, we compared the susceptibility of AID Tg mice to tumorigenesis in the presence or absence of TAA-mediated hepatic inflammation.

To examine whether AID expression affected the inflammatory response levels induced by TAA administration, AID Tg mice were treated with low-dose TAA. Histologic examination revealed that mononuclear cell infiltration levels in the liver of TAA-treated AID Tg mice were comparable with those of the TAA-treated WT mice (Figures 1B and 2A). Quantitative RT-PCR analyses revealed upregulation of proinflammatory cytokines in the liver of AID Tg mice to almost the same levels as those in WT mice, except for relatively low IL-1β expression in AID Tg mice administered 0.02% TAA (Figure 2B). Thus, the TAA-mediated inflammatory response levels in the liver tissue did not largely differ between WT and AID-expressing mice.

Furthermore, consistent with the previous study (24), prominin 1 expression levels were significantly and dose-dependently increased by TAA administration in the liver of both WT and AID Tg mice (Supplementary Figure 3A). No apparent fibrosis was detected by Masson's trichrome stain in mice with and without 0.01% TAA treatment at the end of the 6-month observation period, whereas 0.02% TAA treatment caused minimum fibrotic change in both WT and AID Tg mice (Supplementary Figure 3B).

On the other hand, the livers of AID Tg mice treated with low-dose TAA were enlarged with weights 1.4 to 2.0-fold greater than those of WT mice after 6 months of TAA treatment (Figure 2C). Although previous studies demonstrated that TAA administration at a conventional dose (≥0.03%) caused liver tumors at high rates in rodents (24,26), we found that low-dose TAA administration for 6 months rarely led to the development of liver tumors in WT mice (Table 1). Surprisingly, all the AID Tg mice treated with either 0.01% or 0.02% TAA developed multiple macroscopic hepatic tumors within 6 months (Figure 2D, Table 1), in contrast to findings in WT mice treated with TAA or in AID Tg mice without TAA treatment during the same period. Histologic examination revealed that findings of all liver tumors developing in TAA-treated AID Tg mice were consistent with HCC (Figure 2E), and neither lymphoma nor

cholangiocarcinoma were observed in the liver of those mice. These findings indicated that AID expression concurrent with hepatic inflammation induced by low-dose TAA administration significantly increased the risk of tumor formation compared to AID expression alone or low-dose TAA-induced inflammation alone in liver tissues.

AID-mediated mutagenesis was enhanced by hepatic inflammation

Constitutive AID expression could cause the accumulation of genetic aberrations, and low-dose TAA treatment enhanced tumorigenesis in AID-expressing liver; therefore, we hypothesized that minimal inflammation induced by low-dose TAA accelerated the accumulation of genetic alterations mediated by AID genotoxic activity. We therefore performed whole exome sequencing of tumorous and nontumorous liver tissues obtained from one representative AID Tg mouse with TAA administration and compared the findings with those of a Tg littermate without TAA treatment. As a control, we also performed whole exome sequencing of the liver of their WT littermates with or without TAA administration. We obtained ~1.5 Gb of sequence data per sample on average, and accordingly a total of ~800 Mb of the reads were aligned to the target exons (Supplementary Table 4). The variant filtering process is summarized in Supplementary Figure 1. We identified four somatic mutations in the liver tissue of TAA-treated WT mice, suggesting that low-dose TAA administration *per se* had limited genotoxicity to mouse liver (Supplementary Table 5). On the other hand, whole exome sequencing revealed an accumulation of 22 somatic mutations in the liver of AID Tg mouse without TAA treatment, indicating that the mutagenic activity of AID caused somatic mutations in various genes in the liver tissue. Interestingly, a total of 40 and 416 somatic mutations were accumulated in the nontumorous and tumorous liver tissues of the AID Tg mouse treated with low-dose TAA, respectively. We also confirmed that low-dose TAA treatment did not significantly increase AID expression in the liver tissues of WT mice (Supplementary Figure 4). These findings suggested that administration of low-dose TAA and the resultant hepatic

inflammation enhanced the susceptibility to AID-mediated mutagenesis without affecting AID expression levels.

Mutagenesis induced by AID depends on the transcriptional levels of the target genes in B lymphocytes (27,28). Thus, it is reasonable to assume that transcriptional upregulation induced by TAA-mediated hepatic inflammation facilitated the accumulation of AID-mediated mutagenesis in the liver tissue. To verify this hypothesis, we analyzed the gene expression profiles of liver tissues from WT and AID Tg mice with or without low-dose TAA using a comprehensive cDNA microarray analysis. Of the 39,430 genes analyzed, we identified 223 genes commonly upregulated in the TAA-treated livers of both WT and AID Tg mice (Supplementary Table 6). Pathway analyses using Kyoto Encyclopedia of Genes and Genomes (KEGG; http://www.genome.jp/kegg/) revealed that 98 of 223 (43.9%) upregulated genes were categorized into the well-known signalling pathways, including 16 putative tumor suppressor genes and 8 genes associated with carcinogen metabolism (Supplementary Table 7). Interestingly, three putative tumor suppressor genes, *dual specificity phosphatase 6* (*Dusp6*), *early growth response 1* (*Egr1*) and *inhibitor of DNA binding 2* (*Id2*), which were transcriptionally upregulated in response to low-dose TAA treatment were identified by whole exome sequencing as genes mutated in the tumorous tissue of the TAA-treated AID Tg mouse.

Inflammation-mediated transcriptional upregulation accelerated the accumulation of genetic alterations in tumor-related genes

Transcriptional upregulation of *Dusp6*, *Egr1* and *Id2* in TAA-treated mice was further validated by quantitative RT-PCR, and we confirmed that the transcriptional levels of *Dusp6*, *Egr1* and *Id2* were commonly enhanced in the liver of both WT and AID Tg mice treated with low-dose TAA (Figure 3A). To evaluate the association between transcriptional activation and enhanced accumulation of somatic mutations, we performed additional deep sequencing analyses of *Dusp6*, *Egr1* and *Id2* genes from the livers of WT or AID Tg mice with or without

TAA treatment. Tissue specimens from mice other than those analyzed by whole exome sequencing were subjected to deep sequencing of the selected genes and a 496-fold mean coverage was achieved for the target regions. As for the *Dusp6* gene, numbers of nucleotide alterations accumulated in both tumorous and nontumorous liver tissues of the TAA-treated AID Tg mice (Figure 3B, Supplementary Table 8). Furthermore, several nonsynonymous mutations were shared by tumorous and nontumorous tissues of the same mice, and some of them were predicted to be damaging by in silico analyses using the Sorting Intolerant From Tolerant (SIFT) algorithm (http://provean.jcvi.org/index.php). In contrast to the TAA-treated AID Tg mice, none of the somatic mutations was detectable in the liver of WT mice with or without TAA treatment, and only one nucleotide alteration was detected in AID Tg mice without TAA treatment (Figure 3B). Similarly, the *Egr1* gene commonly acquired numbers of somatic mutations, including nonsynonymous and damaging mutations, in both tumor and nontumorous liver tissues of the TAA-treated AID Tg mice, while no nucleotide alterations were found in the *Egr1* gene in the liver of WT mice with or without TAA treatment, and only one mutation was identified in the *Egr1* gene in AID Tg mice without TAA treatment (Figure 3C, Supplementary Table 8). A similar tendency was confirmed in the *Id2* gene (Figure 3D, Supplementary Table 8). These findings suggested that tumor suppressor genes that were transcriptionally upregulated in the inflamed tissues were predisposed to mutagenesis under AID-expressing conditions.

To further verify the inflammation-associated enhancement of mutagenesis mediated by AID activity, we determined mutational patterns and motifs around the mutated bases. Most mutations (93.6%) observed in the nontumorous liver tissues of AID Tg mice with or without TAA were C to T (or G to A) transitions, which are typical footprints caused by the cytidine deamination activity (Supplementary Table 8). In addition, sequence motifs around the mutated C (and its inverse G) mostly correspond to the DNA sequence WRCH (W = A or T, R = A or G

and H = A or C or T) (29,30), which is a hotspot for AID-mediated mutagenesis (Figures. 3B, 3C, and 3D, right panels).

Finally, to validate the enhanced mutagenesis of the *Dusp6*, *Egr1* and *Id2* genes in the chronically inflamed liver of AID Tg mice, we additionally determined the sequences of these three genes in at least 40 randomly selected clones amplified from the livers of WT or AID Tg mice with or without TAA treatment using conventional sequencing analyses. In agreement with the deep sequencing results, nucleotide alterations were rarely detected (<1 substitutions per 10^4 nucleotides) in the liver of WT mice with or without TAA treatment (Table 2). In contrast to WT mice, AID-expressing liver accumulated mutations of the three genes (1.72-7.73 substitutions per 10^4 nucleotides), and the mutation frequency of all three genes was enhanced by TAA treatment (3.49-13.16 substitutions per 10^4 nucleotides, Table 2). Moreover, all mutations except one deletion in the *Egr1* gene, observed in the liver of AID Tg mice with or without TAA treatment were single nucleotide alterations at C or G sites, predominantly causing C to T (or G to A) transitions (Table 2). Sequence motifs around the mutated bases mostly corresponded to the DNA sequence WRCH, the hot-spot motif of AID-mediated mutagenesis (Figures. 4A, 4B, and 4C).

Taken together, these findings suggested that transcriptional upregulation of tumor-suppressor genes under inflammatory conditions enhanced the accumulation of genetic aberrations mediated by the cytidine deamination activity of AID.

Discussion

Inflammation contributes to cancer development through various mechanisms, such as enhancement of cell growth, induction of angiogenesis and inhibition of apoptosis (2,3). We previously revealed that an intrinsic DNA mutator enzyme, AID, is ectopically expressed under inflammatory conditions in response to proinflammatory cytokine stimulation via the NF-κB dependent pathway (12,31). Although Tg mice with constitutive AID expression developed various tumors, including liver cancers, via the accumulation of somatic mutations of various cancer-related genes (17,25), constitutive AID expression *per se* in epithelial organs requires long periods of time (over a year) to achieve tumorigenesis (25). In the present study, we demonstrated that hepatic inflammation concurrent with constitutive AID expression markedly accelerated tumorigenesis via the enhanced accumulation of somatic mutations in the liver tissues without further enhancing AID expression. These data suggest the presence of mechanisms other than AID induction for mutagenesis accelerated by inflammation.

TAA is a hepatotoxic compound that causes liver tumors at high rates in rodents when administered at a concentration ≥ 0.03% (24,32). In contrast, low-dose (0.01% or 0.02%) TAA administration elicited only a minimal hepatic inflammatory response with a marginal ALT elevation and caused limited liver tumors in WT mice. In sharp contrast to the WT mice, all the AID Tg mice treated with low-dose TAA developed multiple macroscopic liver tumors with histologic features of well- or moderately-differentiated HCC during the 6-month follow-up. On the other hand, none of the AID Tg mice without TAA treatment showed tumorigenesis in the same period. These findings suggested that minimal hepatic inflammation remarkably accelerated tumorigenesis in AID-expressing liver tissues. Since AID expression mediates stepwise genotoxicity that recapitulates human hepatitis-associated carcinogenesis, we hypothesized that minimal hepatic inflammation enhanced the accumulation of genetic alterations triggered by the cytidine deamination activity of AID. Consistent with our hypothesis, whole exome sequencing clarified that the total number of mutated genes in nontumorous liver

of TAA-treated AID Tg mouse was higher than that of TAA-untreated AID Tg mouse. In contrast, TAA treatment alone caused the emergence of a marginal number of mutations in control WT liver tissues. These results indicate that minimal inflammation induced by low-dose TAA administration, which *per se* had little genotoxicity and tumorigenicity in WT mice, accelerated the accumulation of somatic mutations followed by marked hepatocarcinogenesis in AID-expressing liver.

Some assumptions can be made about the mechanisms of enhanced mutagenesis in AID-expressing liver concurrent with minimal inflammation. Although AID expression is known to be elicited by inflammatory response, we confirmed that minimal inflammation induced by low-dose TAA treatment did not alter AID expression in the liver tissues. Thus, hepatic inflammation should have contributed to enhanced mutagenesis through the mechanisms other than affecting AID expression. It has been demonstrated that AID preferentially induces somatic mutations in the actively-transcribed genes, as AID likely attacks the single-strand DNA exposed during the transcription process (27,28,33). Consistently, several previous studies using reporter gene assays and comparative genomics clearly demonstrated that mutation rates increased in a transcription-dependent manner (34,35). Thus, it is reasonable to assume that persistent inflammatory responses induced by low-dose TAA treatment caused transcriptional upregulation of various putative genes targeted by genotoxic activity of AID. Microarray analyses revealed that several genes, including tumor suppressor genes, were transcriptionally upregulated in the liver of AID Tg mice with TAA compared to those without TAA treatment. Transcriptional upregulation of tumor suppressor genes under inflammatory conditions is evidenced by previous findings, such as activation of the *p53* pathway as an intrinsic protective response to minimize cellular damage induced by inflammation (36). Our present findings, however, indicate that the transcriptional upregulation of tumor suppressor genes paradoxically facilitates the acquisition of genetic alterations mediated by AID activity. Indeed, expressions of the putative tumor suppressor genes, *Dusp6*,

Egr1 and *Id2*, were upregulated in the inflamed liver of both WT and AID Tg mice treated with TAA, consistent with the previous studies showing that the *Dusp6*, *Egr1* and *Id2* genes were upregulated in response to stimulation by proinflammatory cytokines, such as TNF-α (37–39). Moreover, both deep sequencing and Sanger sequencing confirmed that these genes accumulated somatic mutations at higher frequencies in TAA-treated AID Tg mice compared to AID Tg mice without TAA administration. Recent studies have shown that mutational signatures of a substituted nucleotide and its flanking sequences strongly reflect underlying mutational process or etiology (40,41). We found that the mutational signatures of the *Dusp6*, *Egr1* and *Id2* genes detected in TAA-treated AID Tg mice are typical footprints of AID-mediated mutagenesis, indicating that the somatic mutations that accumulated in these tumor suppressor genes were caused by the cytidine deamination activity of AID. Taken together, our results suggest that inflammation induced by low-dose TAA administration facilitated the mutagenic effects of AID at least in part via transcriptional upregulation.

Dusp6 is a member of the family of mitogen-activated protein kinase (MAPK) phosphatases and it specifically dephosphorylates and inactivates extracellular-signal-regulated kinase (ERK), acting as a negative regulator of ERK signaling pathways (42). Consistently, inactivation of *Dusp6* in association with cancer progression is reported in various human cancers (43). *Egr1* is a transcription factor with DNA binding function that directly regulates transcription of many tumor suppressor genes, including *Trp53* (44). Thus, *Egr1* is considered to work as a tumor suppressor gene in various cancers, including HCC (45,46). *Id2* is a DNA-binding protein inhibitor family member that dominant-negatively inhibits the functions of basic helix-loop-helix transcription factors (47). Dysregulation of *Id2* is observed in hepatitis C virus-related HCC and is associated with HCC progression (48). Moreover, a subset of human cancers, including HCC, possesses single nucleotide variations of these tumor suppressor genes (International Cancer Genome Consortium data set version 18; http://dcc.icgc.org/web/). Thus, it is tempting to assume that accumulation of somatic mutations in those tumor-related genes are

involved in the enhanced development of HCC in AID-expressing liver concurrent with hepatic inflammation. Because somatic mutations in the *Id2* gene are limited to a relatively small proportion of tumor cells, further analysis is required to determine whether those genetic changes contribute to hepatocarcinogenesis.

It must be noted that only a subset of the upregulated genes determined by microarray analyses acquired somatic mutations in AID-expressing liver with hepatic inflammation. Previous studies clearly revealed that AID has the potential to broadly trigger mutations in nonimmunoglobulin genes including various tumor-related genes. On the other hand, a majority of the nonimmunoglobulin genes targeted by AID are efficiently repaired by DNA repair system, and approximately 25% of the transcriptionally active genes that were not fully protected by repair system acquired mutations in germinal center B cell (49). Thus, it is possible to assume that a subset of the upregulated genes that could not undergo the efficient repair of AID-induced deamination accumulated somatic mutations in the inflamed liver of AID Tg mice. Furthermore, the mutagenic activity of AID is influenced by multiple underlying mechanisms, such as a high transcription rate as well as the presence of AID-associated transcription factor binding sites, including E-box motifs, C/EBP-β binding sites and YY1 binding sites, in the target gene sequences (50). Consistent with those findings, we confirmed that E-box motifs, C/EBP-β binding sites and YY1 binding sites are enriched in the 2-kb region around the transcription start sites of the *Dusp6*, *Egr1* and *Id2* genes (data not shown). Based on these findings, the target genes that accumulate mutations during the inflammation-associated tumorigenesis might share several features, including a high transcription rate and insufficiency of DNA repair mechanisms under inflammatory conditions, and binding sites for specific transcription factors.

In conclusion, we demonstrated that persistent hepatic inflammation accelerated hepatocarcinogenesis by enhancing accumulation of genetic alterations mediated by the cytidine deamination activity of AID. Various tumor suppressor genes were transcriptionally upregulated under inflammatory conditions, thereby enhancing the accumulation of somatic mutations

mediated by AID in a transcription-associated manner. These findings provide the genetic basis for the development of HCC in the background of hepatic inflammation, as human HCC inevitably arises in the inflamed liver underlying chronic hepatitis and/or cirrhosis. Inflammation may have various impacts on key players of mutagenesis, such as DNA repair genes as well as AID, which should be elucidated by further studies.

Supplementary material

Supplementary Tables 1-8 and Figures 1-4 can be found at http://carcin.oxfordjournals.org/

Funding

Japan Society for the Promotion of Science (JSPS) KAKENHI (26293172); Grants-in-aid for Scientific Research on Innovative Areas from the Ministry of Education, Culture, Sports Science and Technology (MEXT) of Japan (22114006); Health Labour Sciences Research Grants from the Ministry of Health, Labour and Welfare of Japan (H26-KANEN); Grant-in-Aid for JSPS Fellows (26.2212).

Acknowledgements

We thank Dr. T. Honjo for the generous donation of AID Tg mice, and Dr. K. Kinoshita for helpful comments.

Conflict of Interest Statement: None declared.

References

1. Hanahan, D. *et al.* (2011) Hallmarks of cancer: the next generation. *Cell*, **144**, 646–674.

2. Grivennikov, S.I. *et al.* (2010) Immunity, inflammation, and cancer. *Cell*, **140**, 883–899.

3. Chiba, T. *et al.* (2012) Inflammation-associated cancer development in digestive organs: mechanisms and roles for genetic and epigenetic modulation. *Gastroenterology*, **143**, 550–563.

4. Weaver, J.M.J. *et al.* (2014) Ordering of mutations in preinvasive disease stages of esophageal carcinogenesis. *Nat. Genet.*, **46**, 837–843.

5. Leedham, S.J. *et al.* (2009) Clonality, founder mutations, and field cancerization in human ulcerative colitis-associated neoplasia. *Gastroenterology*, **136**, 542–550.e6.

6. Ikeda, A. *et al.* (2014) Leptin receptor somatic mutations are frequent in HCV-infected cirrhotic liver and associated with hepatocellular carcinoma. *Gastroenterology*, **146**, 222–232.e35.

7. Shimizu, T. *et al.* (2014) Accumulation of Somatic Mutations in TP53 in Gastric Epithelium With Helicobacter pylori Infection. *Gastroenterology*, **147**, 407–417.e3.

8. Conticello, S.G. (2008) The AID/APOBEC family of nucleic acid mutators. *Genome Biol.*, **9**, 229.

9. Honjo, T. *et al.* (2002) Molecular mechanism of class switch recombination: linkage with somatic hypermutation. *Annu. Rev. Immunol.*, **20**, 165–196.

10. Chaudhuri, J. *et al.* (2004) Class-switch recombination: interplay of transcription, DNA deamination and DNA repair. *Nat. Rev. Immunol.*, **4**, 541–552.

11. Muramatsu, M. *et al.* (2000) Class switch recombination and hypermutation require activation-induced cytidine deaminase (AID), a potential RNA editing enzyme. *Cell*, **102**, 553–563.

12. Matsumoto, Y. *et al.* (2007) Helicobacter pylori infection triggers aberrant expression of activation-induced cytidine deaminase in gastric epithelium. *Nat. Med.*, **13**, 470–476.

13. Endo, Y. *et al.* (2008) Activation-induced cytidine deaminase links between inflammation and the development of colitis-associated colorectal cancers. *Gastroenterology*, **135**, 889–898, 898.e1–3.

14. Komori, J. *et al.* (2008) Activation-induced cytidine deaminase links bile duct inflammation to human cholangiocarcinoma. *Hepatology*, **47**, 888–896.

15. Morita, S. *et al.* (2011) Bile acid-induced expression of activation-induced cytidine deaminase during the development of Barrett's oesophageal adenocarcinoma. *Carcinogenesis*, **32**, 1706–1712.

16. Kou, T. *et al.* (2007) Expression of activation-induced cytidine deaminase in human hepatocytes during hepatocarcinogenesis. *Int. J. Cancer*, **120**, 469–476.

17. Okazaki, I. *et al.* (2003) Constitutive expression of AID leads to tumorigenesis. *J. Exp. Med.*, **197**, 1173–1181.

18. Takai, A. *et al.* (2012) Targeting activation-induced cytidine deaminase prevents colon cancer development despite persistent colonic inflammation. *Oncogene*, **31**, 1733–1742.

19. Matsumoto, T. *et al.* (2006) Expression of APOBEC2 is transcriptionally regulated by NF-kappaB in human hepatocytes. *FEBS Lett.*, **580**, 731–735.

20. Kim, S.K. *et al.* (2014) A model of liver carcinogenesis originating from hepatic progenitor cells with accumulation of genetic alterations. *Int. J. Cancer*, **134**, 1067–1076.

21. Fujiwara, M. *et al.* (2008) Parkin as a tumor suppressor gene for hepatocellular carcinoma. *Oncogene*, **27**, 6002–6011.

22. Nasu, A. *et al.* (2011) Genetic heterogeneity of hepatitis C virus in association with antiviral therapy determined by ultra-deep sequencing. *PLoS One*, **6**, e24907.

23. Nishijima, N. *et al.* (2012) Dynamics of hepatitis B virus quasispecies in association with nucleos(t)ide analogue treatment determined by ultra-deep sequencing. *PLoS One*, **7**, e35052.

24. Sakurai, T. *et al.* (2013) P38A Inhibits Liver Fibrogenesis and Consequent Hepatocarcinogenesis By Curtailing Accumulation of Reactive Oxygen Species. *Cancer Res.*, **73**, 215–224.

25. Morisawa, T. *et al.* (2008) Organ-specific profiles of genetic changes in cancers caused by activation-induced cytidine deaminase expression. *Int. J. Cancer*, **123**, 2735–2740.

26. Yeh, C.N. *et al.* (2004) Thioacetamide-induced intestinal-type cholangiocarcinoma in rat: an animal model recapitulating the multi-stage progression of human cholangiocarcinoma. *Carcinogenesis*, **25**, 631–636.

27. Ramiro, A.R. *et al.* (2003) Transcription enhances AID-mediated cytidine deamination by exposing single-stranded DNA on the nontemplate strand. *Nat. Immunol.*, **4**, 452–456.

28. Sohail, A. *et al.* (2003) Human activation-induced cytidine deaminase causes transcription-dependent, strand-biased C to U deaminations. *Nucleic Acids Res.*, **31**, 2990–2994.

29. Rogozin, I.B. *et al.* (2004) Cutting edge: DGYW/WRCH is a better predictor of mutability at G:C bases in Ig hypermutation than the widely accepted RGYW/WRCY motif and probably reflects a two-step activation-induced cytidine deaminase-triggered process. *J. Immunol.*, **172**, 3382–3384.

30. Meng, F.L. *et al.* (2014) Convergent Transcription at Intragenic Super-Enhancers Targets AID-Initiated Genomic Instability. *Cell*, **159**, 1538–1548.

31. Endo, Y. *et al.* (2007) Expression of activation-induced cytidine deaminase in human hepatocytes via NF-kappaB signaling. *Oncogene*, **26**, 5587–5595.

32. Newell, P. *et al.* (2008) Experimental models of hepatocellular carcinoma. *J. Hepatol.*, **48**, 858–879.

33. Yoshikawa, K. *et al.* (2002) AID enzyme-induced hypermutation in an actively transcribed gene in fibroblasts. *Science*, **296**, 2033–2036.

34. Park, C. *et al.* (2012) Genomic evidence for elevated mutation rates in highly expressed genes. *EMBO Rep.*, **13**, 1123–1129.

35. Beletskii, A. *et al.* (1996) Transcription-induced mutations: increase in C to T mutations in the nontranscribed strand during transcription in Escherichia coli. *Proc. Natl. Acad. Sci. U. S. A.*, **93**, 13919–13924.

36. Staib, F. *et al.* (2005) The p53 tumor suppressor network is a key responder to microenvironmental components of chronic inflammatory stress. *Cancer Res.*, **65**, 10255–10264.

37. Breitschopf, K. *et al.* (2000) Posttranslational modification of Bcl-2 facilitates its proteasome-dependent degradation: molecular characterization of the involved signaling pathway. *Mol. Cell. Biol.*, **20**, 1886–1896.

38. Cao, Y. *et al.* (2013) TNF-α induces early growth response gene-1 expression via ERK1/2 activation in endothelial cells. *Acta Diabetol.*, **50**, 27–31.

39. Tzeng, S. *et al.* (1999) Tumor Necrosis Factor-Alpha Regulation of the Id Gene Family in Astrocytes and Microglia During CNS. *Glia*, **26**, 139–152.

40. Alexandrov, L.B. *et al.* (2013) Signatures of mutational processes in human cancer. *Nature*, **500**, 415–421.

41. Olivier, M. *et al.* (2014) Modelling mutational landscapes of human cancers in vitro. *Sci. Rep.*, **4**, 4482.

42. Owens, D.M. *et al.* (2007) Differential regulation of MAP kinase signalling by dual-specificity protein phosphatases. *Oncogene*, **26**, 3203–3213.

43. Furukawa, T. *et al.* (2005) Distinct progression pathways involving the dysfunction of DUSP6/MKP-3 in pancreatic intraepithelial neoplasia and intraductal papillary-mucinous neoplasms of the pancreas. *Mod. Pathol.*, **18**, 1034–1042.

44. Baron, V. *et al.* (2006) The transcription factor Egr1 is a direct regulator of multiple tumor suppressors including TGFbeta1, PTEN, p53, and fibronectin. *Cancer Gene Ther.*, **13**, 115–124.

45. Hao, M.W. *et al.* (2002) Transcription factor EGR-1 inhibits growth of hepatocellular carcinoma and esophageal carcinoma cell lines. *World J. Gastroenterol.*, **8**, 203–207.

46. Tian, H. *et al.* (2014) Ribonucleotide reductase M2B inhibits cell migration and spreading by early growth response protein 1-mediated phosphatase and tensin homolog/Akt1 pathway in hepatocellular carcinoma. *Hepatology*, **59**, 1459–1470.

47. Perk, J. *et al.* (2005) Id family of helix-loop-helix proteins in cancer. *Nat. Rev. Cancer*, **5**, 603–614.

48. Tsunedomi, R. *et al.* (2006) Identification of ID2 associated with invasion of hepatitis C virus-related hepatocellular carcinoma by gene expression profile. *Int. J. Oncol.*, **29**, 1445–1451.

49. Liu, M. *et al.* (2008) Two levels of protection for the B cell genome during somatic hypermutation. *Nature*, **451**, 841–845.

50. Duke, J.L. *et al.* (2013) Multiple transcription factor binding sites predict AID targeting in non-Ig genes. *J. Immunol.*, **190**, 3878–3888.

Table and Figure Legends

Table 1. Incidence of liver tumors observed in WT and AID Tg mice with and without TAA administration.

Table 2. Gene mutation frequencies in nontumorous liver tissues of WT mice and AID Tg mice with and without TAA treatment.

Fig. 1. Chronic hepatic inflammation induced by low-dose TAA administration in wild-type (WT) mice. (**A**) Time course of changes in serum ALT during TAA administration. Blood samples were repeatedly collected from WT mice administered 0.01%, 0.02% and 0.03% TAA, and their control mice at the indicated time-points. Vertical bars show SD. (**B**) Microscopic (hematoxylin and eosin stain) images of the liver of WT mice with and without TAA administration for 8 weeks. (**C**) Representative results of RT-PCR for the expression of various proinflammatory cytokines in the liver of WT mice with and without 0.02% TAA administration. IL, interleukin. (**D**) Immunostaining images of liver tissue specimens of WT mouse with and without 0.02% TAA administration. Upper, E-cadherin immunofluorescence; Middle, Ki-67 immunofluorescence; Lower, DAPI staining.

Fig. 2. Chronic hepatic inflammation and tumor phenotype induced by TAA administration in AID Tg mice. (**A**) Representative microscopic (hematoxylin and eosin stain) images of the livers of AID Tg mice with and without 0.02% TAA administration for 8 weeks. In AID Tg mice with TAA administration, similar levels of inflammatory cellular infiltration were observed as compared to WT mice treated with TAA (see Figure 1B). (**B**) Cytokine expressions in the liver of WT mice and AID Tg mice with and without TAA administration analyzed by quantitative RT-PCR. Total RNA was isolated from the livers of mice administered TAA at the indicated concentrations. The results were normalized to 18S rRNA expression and are shown as means ± SD values. IL, interleukin. (**C**) Liver weight of WT mice and AID Tg mice after TAA administration for 6 months. Data are means ± SD values. (**D**) Macroscopic images of a

representative liver of WT mouse treated with 0.02% TAA (upper panel) and an AID Tg mouse treated with 0.02% TAA (lower panel). (**E**) Representative microscopic (hematoxylin and eosin stain) images of a liver tumor that developed in an AID Tg mouse treated with 0.02% TAA for 6 months.

Fig. 3. Transcriptional upregulation and accumulation of somatic mutations in *Dusp6*, *Egr1* and *Id2* genes. (**A**) Transcriptional upregulation of *Dusp6*, *Egr1* and *Id2* genes induced by TAA-mediated hepatic inflammation. Total RNA was isolated from the liver of WT and AID Tg mice with or without 0.01% TAA administration, and *Dusp6*, *Egr1* and *Id2* expressions were analyzed by quantitative RT-PCR. The results were normalized to 18S rRNA expression and shown as means ± SD values. NT, nontumor; T, tumor. (**B**, **C** and **D**, left panels) Distribution of mutations in the *Dusp6* (**B**), *Egr1* (**C**) and *Id2* (**D**) genes determined by deep sequencing analyses. Schematic diagrams and mutated nucleotide positions of nontumorous liver tissue of WT and AID Tg mice with or without TAA administration determined by deep sequencing are shown. Black triangles indicate mutated positions in each gene, and asterisks indicate common mutations with those observed in tumorous liver tissues of the same mouse. (**B**, **C** and **D**, right panels) Frequencies of bases at each position around the mutated Cs in nontumorous liver tissues from AID Tg mice with and without TAA treatment. Bases around mutated Gs are shown as complementary bases.

Fig. 4. Mutational signatures of *Dusp6*, *Egr1* and *Id2* genes determined by Sanger sequencing. Representative electropherograms around the mutated Cs of *Dusp6* (**A**), *Egr1* (**B**) and *Id2* (**C**) genes are shown in upper panels. Sequence motifs around the mutated Cs observed in the nontumorous liver tissues of AID Tg mice with TAA treatment are shown in lower panels. Bases around mutated Gs are shown as complementary bases.

Supplementary Table 1. Primer sequences used for quantitative RT-PCR amplification.

Supplementary Table 2. Primer sequences used for deep sequencing analysis.

Supplementary Table 3. Primer sequences used for Sanger sequencing analysis.

Supplementary Table 4. Summary of whole exome sequencing.

Supplementary Table 5. List of somatic mutations detected by whole exome sequencing.

Supplementary Table 6. Genes upregulated by TAA in both WT and AID Tg mice.

Supplementary Table 7. Genes annotated in KEGG pathway database among those upregulated by TAA in both WT and AID Tg mice

Supplementary Table 8. List of somatic mutations detected by deep sequencing.

Supplementary Fig. 1. Variant filtering process for identification of somatic mutations in whole exome sequencing.

Supplementary Fig. 2. Variant filtering process for identification of somatic mutations in deep sequencing of selected genes.

Supplementary Fig. 3. Prominin 1 expression and fibrotic change in the liver tissues of WT mice and AID Tg mice with or without TAA treatment. (**A**) Prominin 1 expression in the liver of WT mice and AID Tg mice with and without TAA administration analyzed by quantitative RT-PCR. Total RNA was isolated from the livers of mice administered TAA at the indicated concentrations. The results were normalized to 18S rRNA expression and are shown as means ± SD values. (**B**) Representative microscopic (Masson's trichrome stain) images of the liver of WT mice and AID Tg mice with and without TAA administration for 6 months.

Supplementary Fig. 4. AID expression in the liver tissues of WT mice and AID Tg mice with or without TAA treatment. Total RNA was isolated from the liver of each mouse, and AID expression was analyzed by quantitative RT-PCR. The results were normalized to 18S rRNA expression and are shown as means ± SD values.

Supplementary Fig. 5. Uncropped gel images of RT-PCRs in Figure 1C.

Figure 1. Matsumoto et al.

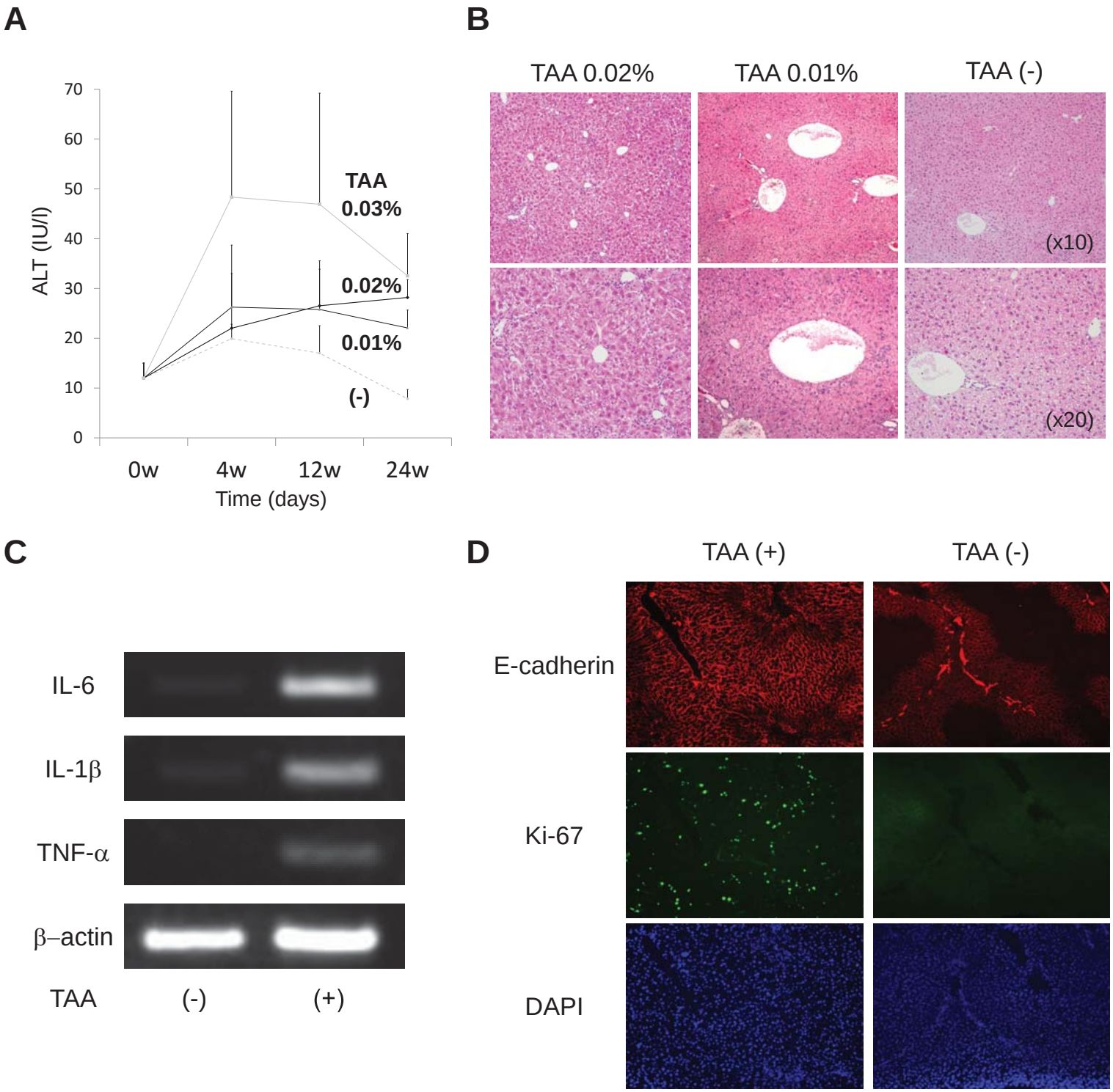

Figure 2. Matsumoto et al.

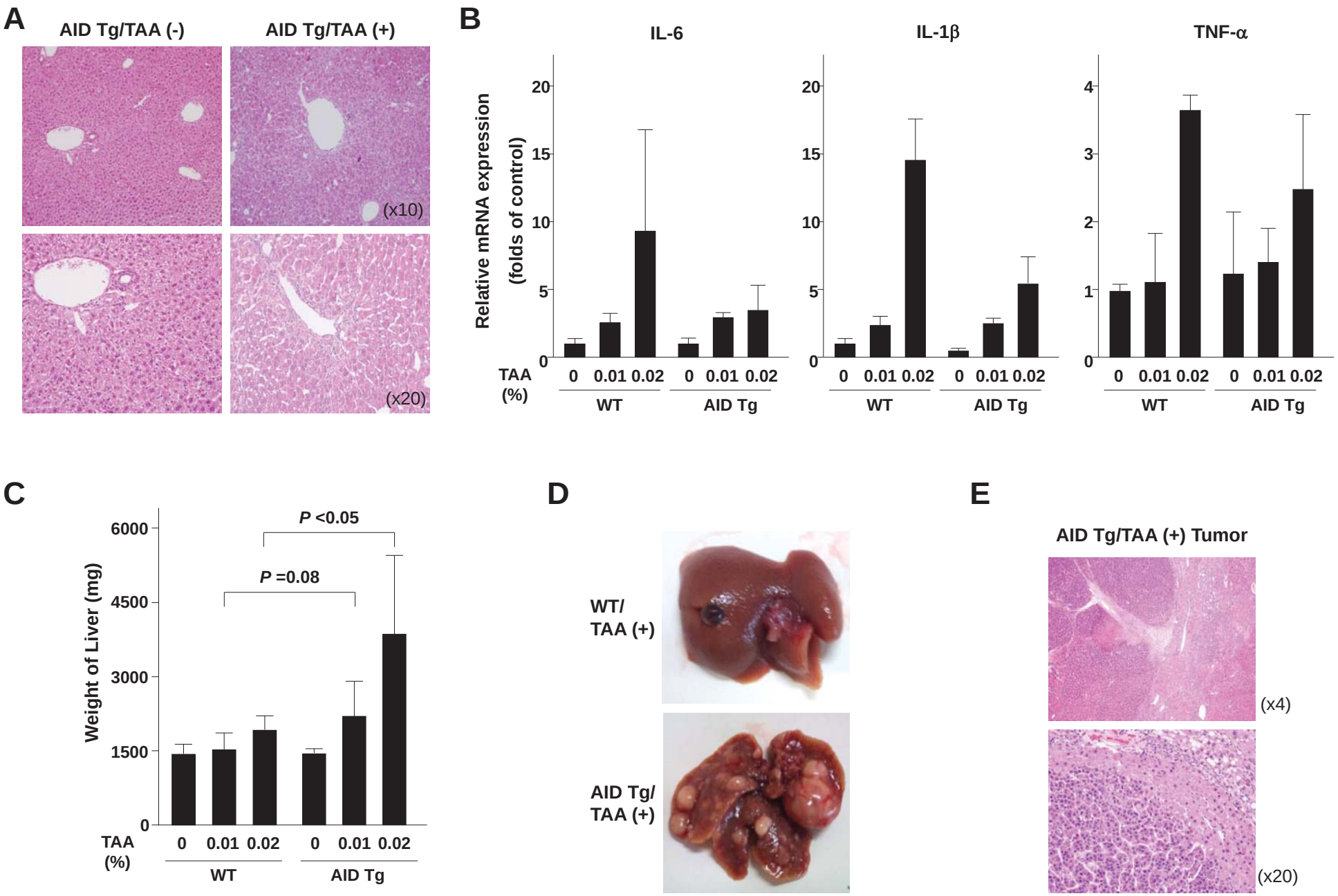

Figure 3. Matsumoto et al.

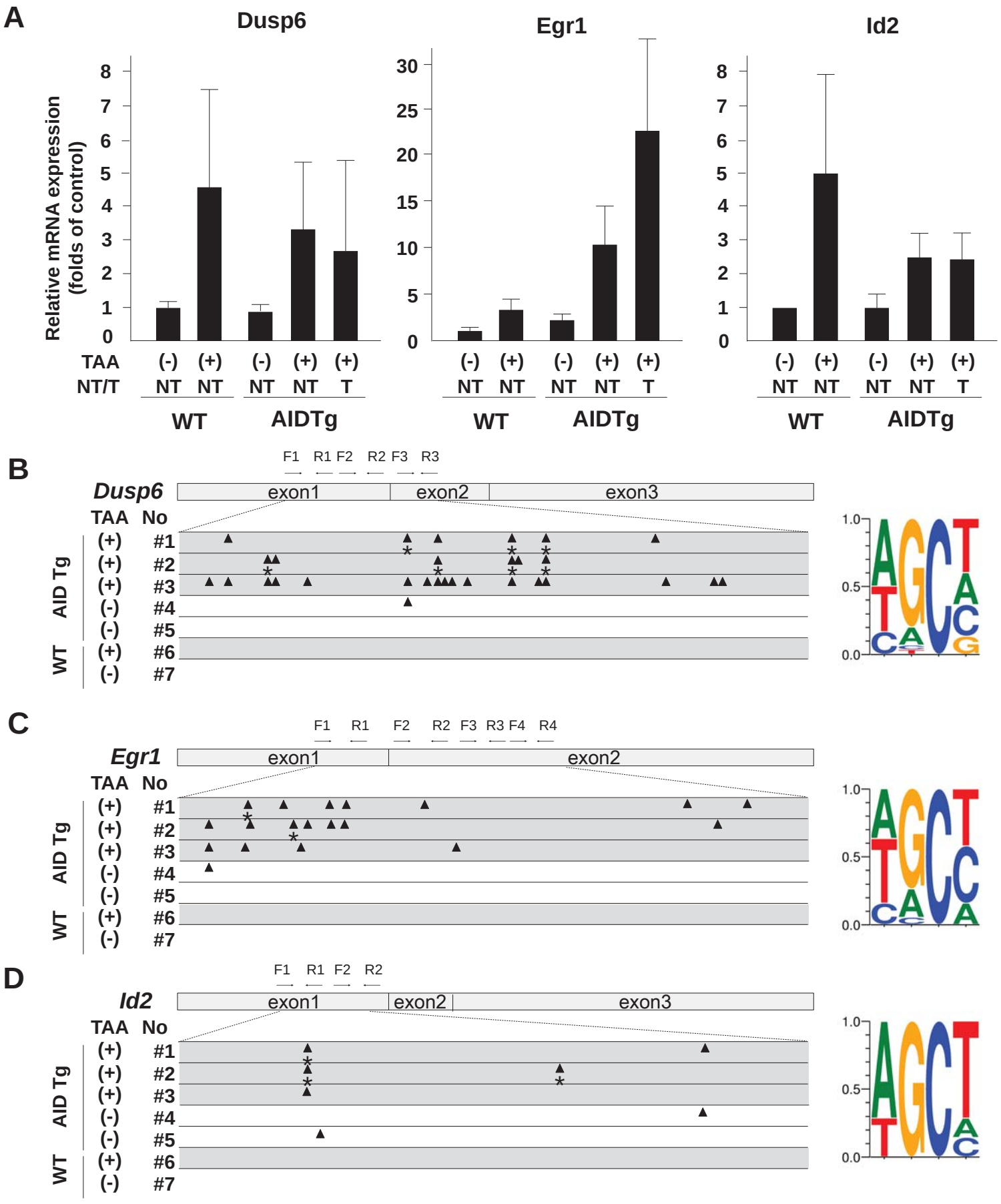

Figure 4. Matsumoto et al.

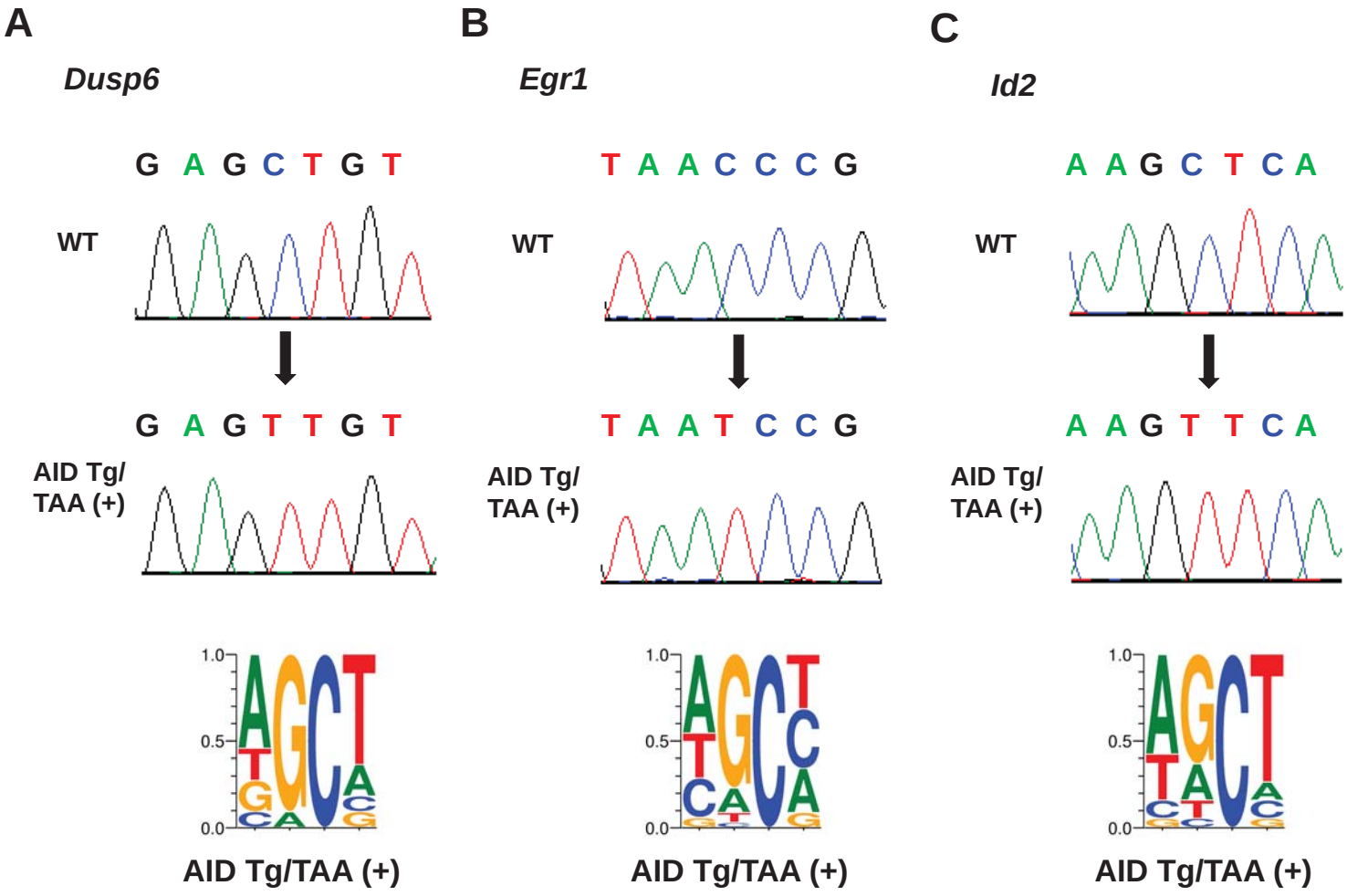

Table 1. Incidence of liver tumors observed in WT and AID Tg mice with and without TAA administration.

		Control		TAA 0.01%		TAA 0.02%	
		WT n=11	AID Tg n=6	WT n=13	AID Tg n=14	WT n=8	AID Tg n=8
Liver tumors	None	11 (100%)	6 (100%)	11 (85%)	0 (0%)	6 (75%)	0 (0%)
	1	0 (0%)	0 (0%)	2 (15%)	0 (0%)	1 (12.5%)	0 (0%)
	2-3	0 (0%)	0 (0%)	0 (0%)	0 (0%)	1 (12.5%)	0 (0%)
	>4	0 (0%)	0 (0%)	0 (0%)	14 (100%)	0 (0%)	8 (100%)

Values in parenthesis show percentages of animals that developed liver tumors.

Table 2. Gene mutation frequencies in nontumorous liver tissues of WT mice and AID Tg mice with and without TAA treatment.

Target gene	Strain	TAA treatment	Mutated clones (n/total)	Mutated nucleotides (n/total bases)	Mutation rate (/10000 bases)	C:T, G:A mutation (n; %)
Dusp6	WT	(-)	2/44	2/31,862	0.63	2 (100%)
	WT	(+)	3/48	3/34,658	0.87	2 (66.7%)
	AID Tg	(-)	4/47	6/34,976	1.72	3 (50.0%)
	AID Tg	(+)	6/43	11/31,546	3.49	8 (72.7%)
Egr1	WT	(-)	1/43	1/23,713	0.42	1 (100.0%)
	WT	(+)	1/46	1/28,270	0.35	1 (100.0%)
	AID Tg	(-)	11/47	21/27,164	7.73	12 (81.0%)
	AID Tg	(+)	15*/44	36/27,349	13.16	33 (91.7%)
Id2	WT	(-)	0/43	0/20,294	0	-
	WT	(+)	0/45	0/21,952	0	-
	AID Tg	(-)	6/46	12/22,347	5.37	9 (75%)
	AID Tg	(+)	10/43	19/21,297	8.92	16 (84.2%)

* One clone had deletion in *Egr1* gene.

Supplementary Figure 1. Matsumoto et al.

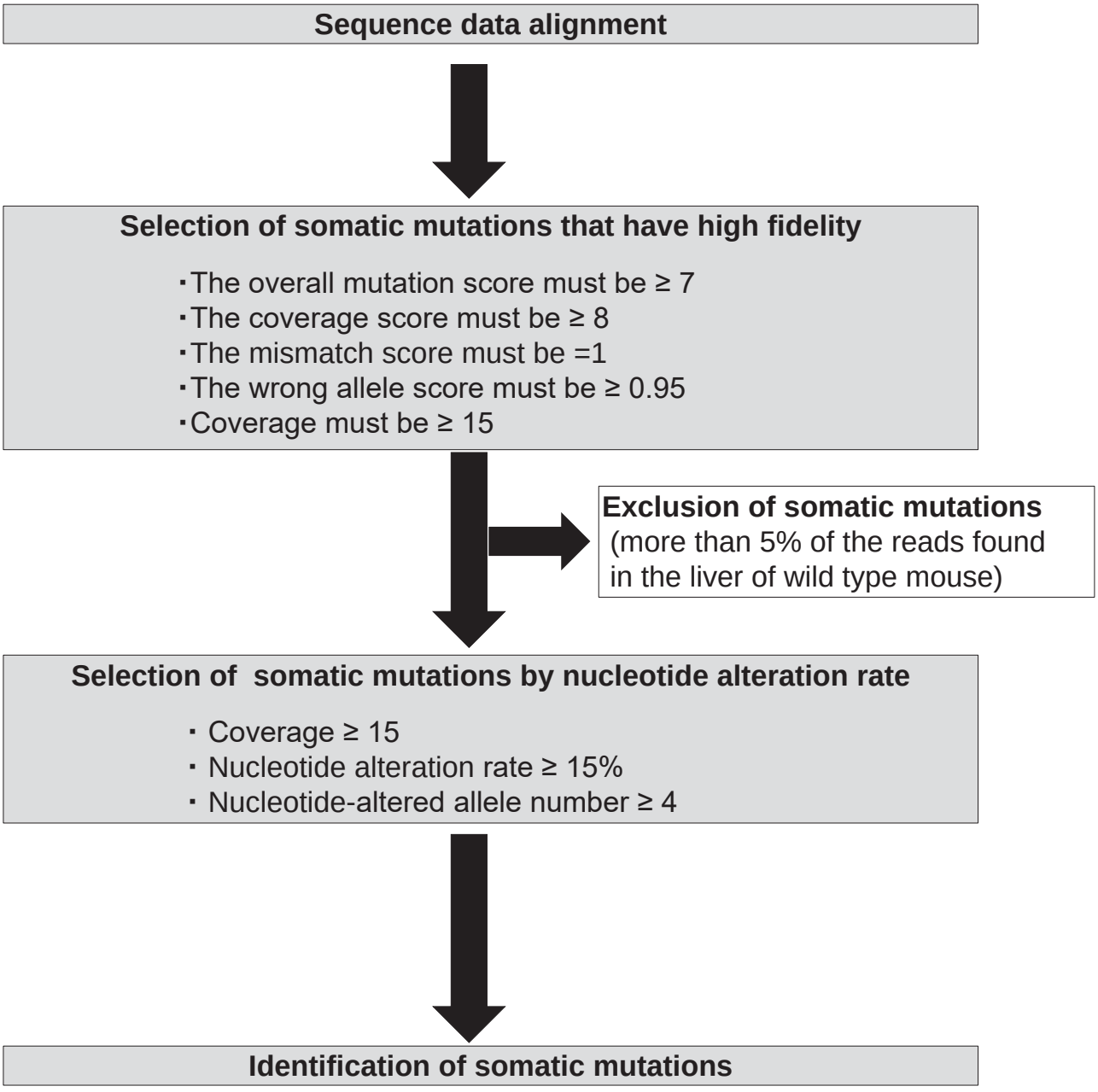

Supplementary Figure 2. Matsumoto et al.

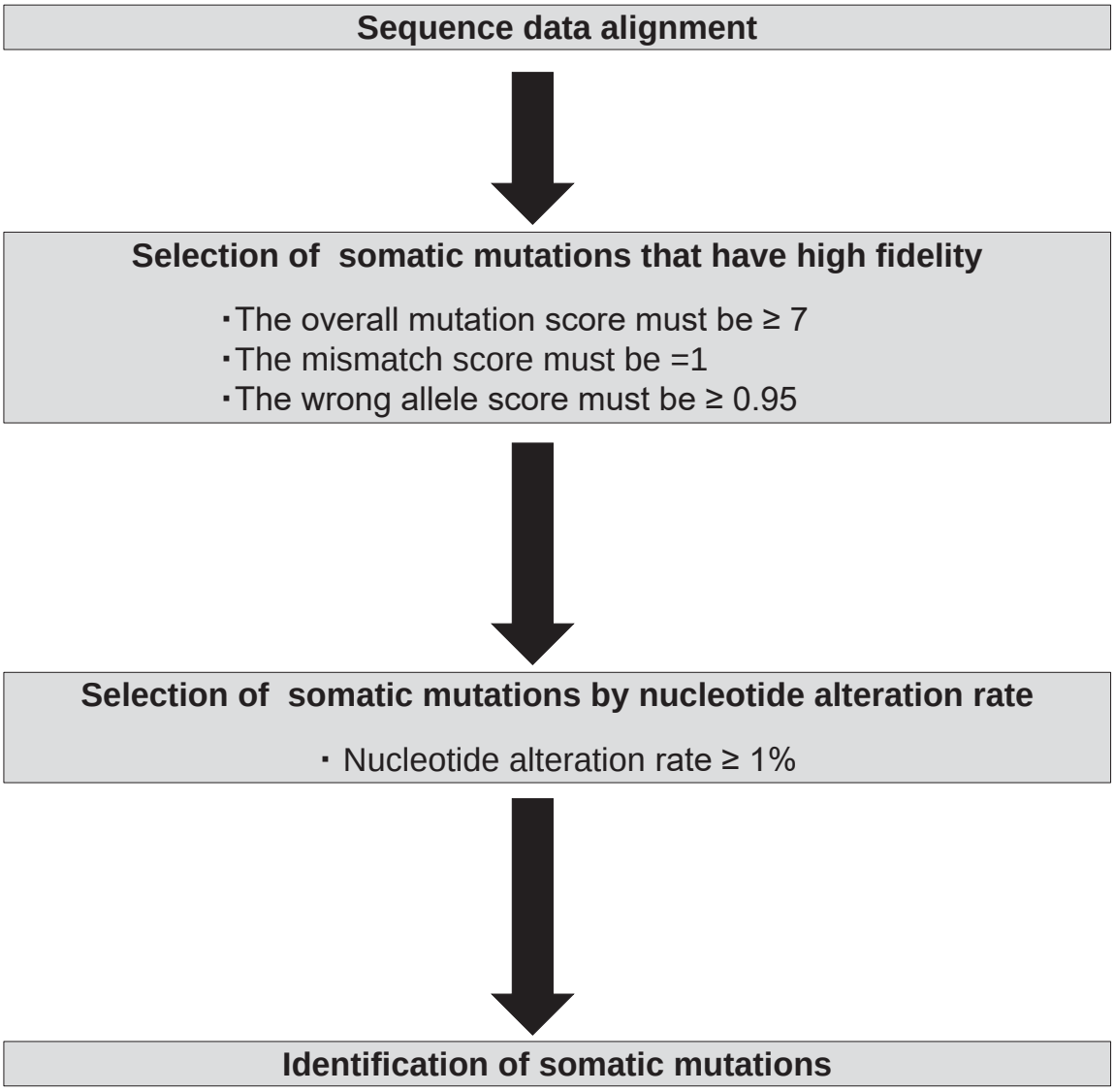

Supplementary Figure 3. Matsumoto et al.

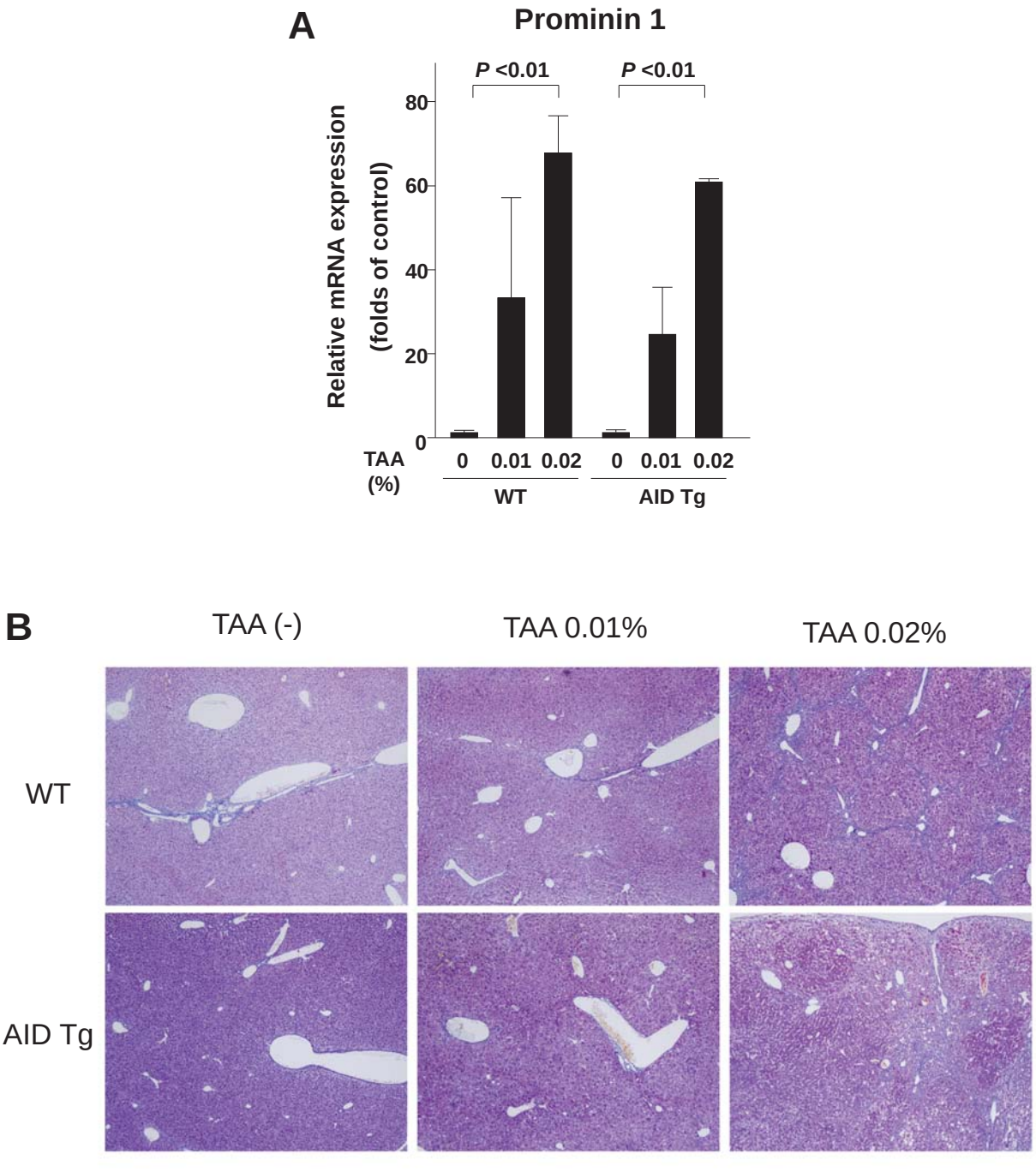

Supplementary Figure 4. Matsumoto et al.

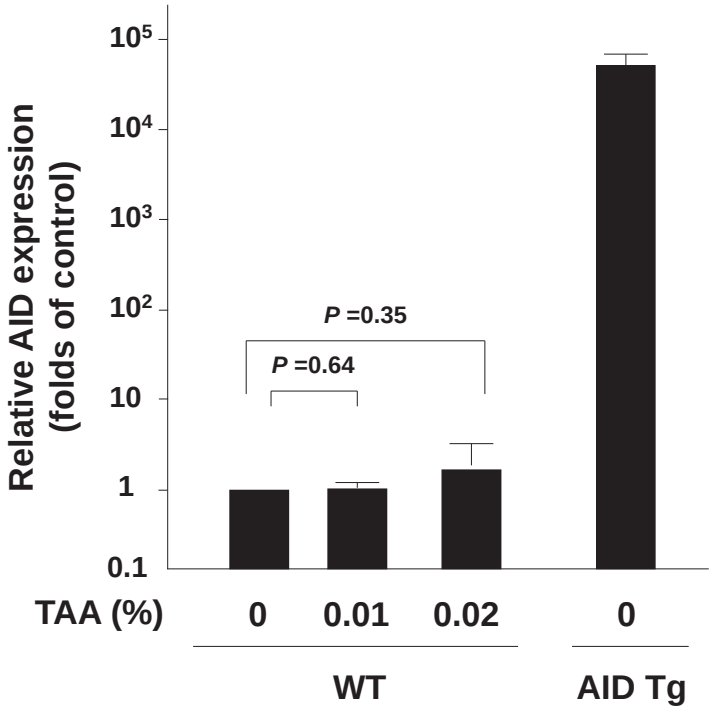

Supplementary Table 1. Primer sequences used for quantitative RT-PCR amplification.

	Forward primer	Reverse primer
IL-6	5'-TCCATCCAGTTGCCTTCTTG-3'	5'-CCACGATTTCCCAGAGAACA-3'
IL-1β	5'-CCTTCCAGGATGAGGACATGAG-3'	5'-GTTGTTCATCTCGGAGCCTGTAG-3'
TNF-α	5'-GACGTGGAACTGGCAGAAGAG-3'	5'-CGATCACCCCGAAGTTCAGTAG-3'
AID	5'-CGTGGTGAAGAGGAGAGATAGT-3'	5'-CAGTCTGAGATGTAGCGTAGGA-3'
Prominin 1	5'-CCAGCGGCAGAAGCAGAATG-3'	5'-CGAGTCCTGGTCTGCTGGTT-3'
Dusp6	5'-CAGCGACTGGAATGAGAACA-3'	5'-CAATGTCCGAGGAAGAGTCC-3'
Id2	5'-ATGAAAGCCTTCAGTCCGGTG-3'	5'-AGCAGACTCATCGGGTCGT-3'
Egr1	5'-TATGAGCACCTGACCACAGAG-3'	5'-GCTGGGATAACTCGTCTCCA-3'
18S rRNA	5'-TAGAGTGTTCAAAGCAGGCCC-3'	5'-CCAACAAAATAGAACCGCGGT-3'

Supplementary Table 2. Primer sequences used for deep sequencing analysis.

	Forward primer	Reverse primer
Dusp6 (1)	5'-CAGCTCGACCCCCATGATAG-3'	5'-CTCGTACAGCTCCTGTGGTC-3'
Dusp6 (2)	5'-CCATTAATGTGGCCATCCCCG-3'	5'-GTTCTCATTCCAGTCGCTGCT-3'
Dusp6 (3)	5'-CAGTAAGTTCCAGGCCGAGT-3'	5'-CCGTTGCACTATTGGGGTCT-3'
Egr1 (1)	5'-AAACTGGAGGAGATGATGCTGC-3'	5'-TCGGCTCCCCTTGAGGATTG-3'
Egr1 (2)	5'-GGAGACGAGTTATCCCAGCC-3'	5'-AGAGGTCGGAGGATTGGTCA-3'
Egr1 (3)	5'-CCAACGACAGCAGTCCCATC-3'	5'-TCATGGGAACCTGGAAACCAC-3'
Egr1 (4)	5'-AACAACAGGGAGACCTGAGC-3'	5'-GAGCTGGGATTGGTAGGTGG-3'
Id2 (1)	5'-CCTCCTACGAGCAGCATGAA-3'	5'-GAGCTTGGAGTAGCAGTCGT-3'
Id2 (2)	5'-ATCCCCCAGAACAAGAAGGTGA-3'	5'-TCCGTGTTCAGGGTGGTCAG-3'

Supplementary Table 3. Primer sequences used for Sanger sequencing analysis.

	Forward primer	Reverse primer
Dusp6	5'-GTTAAGCTTTGACTTCTGTGTCGCTTTCC-3'	5'-GTTGAATTCCACCCTGAACTACGTTTCC-3'
Id2	5'-ATTAAGCTTCGCTTCATTCTGAACCGA-3'	5'-ATTGAATTCTAATGAACCTGTCTCTACGATG-3'
Egr1	5'-ATTAAGCTTAGAGATCCCAGCGCGCAGAA-3'	5'-ATTGAATTCACAAGACCCTGGAGCTGTGTGA-3'

Supplementary Table 4. Summary of whole exome sequencing.

	Bases mapped to targeted regions* (Mbp)	**Median Coverage (Target region)**	**>=1x coverage (%)**	**>=10x coverage (%)**	**>=20x coverage (%)**	**>=30x coverage (%)**
WT without TAA (nontumor)	667.4	18.78	74.57	55.92	37.00	22.39
WT with TAA (nontumor)	1294.0	37.61	82.13	67.64	59.94	49.23
AID Tg without TAA (nontumor)	755.9	21.27	78.09	58.14	39.21	24.91
AID Tg with TAA (nontumor)	703.7	19.80	77.12	61.40	40.12	23.63
AID Tg with TAA (tumor)	599.9	16.88	76.51	40.55	25.95	17.69

*Targeted bases for analyses were 35.53 Mbp.

Supplementary Table 5. List of somatic mutations detected by whole exome sequencing.

Strain	TAA	T or NT*	Gene	Chr**	Chr** Position	Coverage	Reference Nucleotide	Mutation Nucleotide	Mutant allele frequency (%)	Mutant allele number	Mutation type***
WT	(+)	NT	9430031J16Rik	1	81265744	264	G	A	20.08	53	SNV
WT	(+)	NT	6330416G13Rik	4	63229601	39	T	Del	15.38	6	indel
WT	(+)	NT	Muc19	15	91739233	47	A	C	19.15	9	SNV
WT	(+)	NT	Zfp641	15	98119213	53	T	G	15.09	8	SNV
AIDTg	(-)	NT	Inpp4a	1	37435861	34	G	C	17.65	6	SNV
AIDTg	(-)	NT	Ada	2	163556963	43	A	C	16.28	7	SNV
AIDTg	(-)	NT	Mmp9	2	164775500	21	A	C	19.05	4	SNV
AIDTg	(-)	NT	Slc2a10	2	165340637	42	T	G	19.05	8	SNV
AIDTg	(-)	NT	Tnrc4	3	94289472	31	A	C	19.35	6	SNV
AIDTg	(-)	NT	Ptprf	4	117908555	30	T	G	20	6	SNV
AIDTg	(-)	NT	Cdc20	4	118105618	23	C	T	17.39	4	SNV
AIDTg	(-)	NT	Psmc2	5	21302430	19	A	C	21.05	4	SNV
AIDTg	(-)	NT	Letm1	5	34112030	23	T	G	21.74	5	SNV
AIDTg	(-)	NT	Smr3a	5	88437345	31	G	C	16.13	5	SNV
AIDTg	(-)	NT	Fbxo41	6	85428600	26	A	C	15.38	4	SNV
AIDTg	(-)	NT	Cidec	6	113375584	96	A	G	20.83	20	SNV
AIDTg	(-)	NT	Lysmd4	7	74371100	37	T	G	16.22	6	SNV
AIDTg	(-)	NT	Gpr114	8	97458362	26	T	G	19.23	5	SNV
AIDTg	(-)	NT	Dpep2	8	108512013	40	T	G	15	6	SNV
AIDTg	(-)	NT	Adamts7	9	90091929	66	G	T	18.18	12	SNV
AIDTg	(-)	NT	Aoc3	11	101192411	50	A	C	16	8	SNV
AIDTg	(-)	NT	Klhl38	15	58153619	36	T	G	22.22	8	SNV
AIDTg	(-)	NT	Dtx3l	16	35932521	42	G	T	19.05	8	SNV
AIDTg	(-)	NT	Galm	17	80582534	21	T	G	19.05	4	SNV
AIDTg	(-)	NT	Lrp5	19	3659280	39	T	G	15.38	6	SNV
AIDTg	(-)	NT	Cstf2t	19	31159250	20	A	G	20	4	SNV
AIDTg	(+)	NT	G0s2	1	195098888	23	G	A	21.74	5	SNV
AIDTg	(+)	NT	Ntng2	2	29083641	27	G	T	22.22	6	SNV
AIDTg	(+)	NT	Car13	3	14650703	50	T	G	16	8	SNV
AIDTg	(+)	NT	Gm128	3	95044785	21	A	C	19.05	4	SNV

AIDTg	(+)	NT	Rbm15	3	107133636	24	G	T	16.67	4	SNV
AIDTg	(+)	NT	Fam73a	3	151939741	26	T	C	15.38	4	SNV
AIDTg	(+)	NT	Abca1	4	53084729	25	G	T	16	4	SNV
AIDTg	(+)	NT	Spen	4	141034413	25	T	G	20	5	SNV
AIDTg	(+)	NT	Speer4c	5	15029386	33	T	C	24.24	8	SNV
AIDTg	(+)	NT	Psmc2	5	21302430	25	A	C	24	6	SNV
AIDTg	(+)	NT	Adam1a	5	121971216	31	T	C	16.13	5	SNV
AIDTg	(+)	NT	Eln	5	135205268	35	A	C	17.14	6	SNV
AIDTg	(+)	NT	Flt3	5	148146493	26	A	C	15.38	4	SNV
AIDTg	(+)	NT	Brca2	5	151359484	37	T	G	21.62	8	SNV
AIDTg	(+)	NT	Cidec	6	113375584	64	A	G	15.62	10	SNV
AIDTg	(+)	NT	Ncapd2	6	125123099	35	A	C	20	7	SNV
AIDTg	(+)	NT	Ptpro	6	137316619	31	T	G	16.13	5	SNV
AIDTg	(+)	NT	Zfp382	7	30918935	16	G	T	25	4	SNV
AIDTg	(+)	NT	Plekhf1	7	39006484	18	G	T	22.22	4	SNV
AIDTg	(+)	NT	Nup62-il4i1	7	52095895	16	G	T	25	4	SNV
AIDTg	(+)	NT	Herc2	7	63402028	21	A	C	19.05	4	SNV
AIDTg	(+)	NT	Muc5ac	7	149004698	31	C	A	19.35	6	SNV
AIDTg	(+)	NT	Muc5ac	7	149004701	32	A	T	18.75	6	SNV
AIDTg	(+)	NT	Nfix	8	87240157	25	C	A	16	4	SNV
AIDTg	(+)	NT	Sall1	8	91556705	15	C	A	26.67	4	SNV
AIDTg	(+)	NT	Nfrkb	9	31208219	25	T	G	16	4	SNV
AIDTg	(+)	NT	Hdac2	10	36708998	23	T	G	17.39	4	SNV
AIDTg	(+)	NT	Mcm9	10	53283209	26	G	C	15.38	4	SNV
AIDTg	(+)	NT	Apc2	10	79768978	22	G	T	22.73	5	SNV
AIDTg	(+)	NT	Ankrd52	10	127825686	24	A	C	16.67	4	SNV
AIDTg	(+)	NT	Dnahc2	11	69262081	20	T	C	20	4	SNV
AIDTg	(+)	NT	Ston2	12	92886834	44	T	G	20.45	9	SNV
AIDTg	(+)	NT	Ucn3	13	3940460	26	A	C	15.38	4	SNV
AIDTg	(+)	NT	Hfe	13	23797765	17	T	G	23.53	4	SNV
AIDTg	(+)	NT	Hivep1	13	42255411	26	T	C	19.23	5	SNV
AIDTg	(+)	NT	Rbm26	14	105550576	53	T	G	15.09	8	SNV
AIDTg	(+)	NT	Rnf19a	15	36175311	37	A	C	18.92	7	SNV
AIDTg	(+)	NT	LOC100502698	16	32844648	43	A	G	16.28	7	SNV
AIDTg	(+)	NT	Qtrtd1	16	43881270	40	A	C	15	6	SNV

AIDTg	(+)	NT	Rfx2	17	56927145	20	A	C	20	4	SNV
AIDTg	(+)	T	Sulf1	1	12787024	22	G	T	18.18	4	SNV
AIDTg	(+)	T	Crispld1	1	17752275	31	A	C	16.13	5	SNV
AIDTg	(+)	T	Crispld1	1	17752276	30	A	T	16.67	5	SNV
AIDTg	(+)	T	Pkhd1	1	20559966	20	A	T	25	5	SNV
AIDTg	(+)	T	Prim2	1	33511006	27	C	A	18.52	5	SNV
AIDTg	(+)	T	Prim2	1	33511008	27	T	A	18.52	5	SNV
AIDTg	(+)	T	Tmem131	1	36938219	28	T	A	17.86	5	SNV
AIDTg	(+)	T	Inpp4a	1	37424643	16	A	T	25	4	SNV
AIDTg	(+)	T	Dytn	1	63721483	25	G	A	24	6	SNV
AIDTg	(+)	T	Ugt1a1	1	90108830	49	T	Del	20.41	10	indel
AIDTg	(+)	T	Sh3bp4	1	91041388	20	A	Del	20	4	indel
AIDTg	(+)	T	Cops8	1	92503183	22	T	G	22.73	5	SNV
AIDTg	(+)	T	Cops8	1	92506690	25	T	Del	16	4	indel
AIDTg	(+)	T	Hes6	1	93308746	21	G	A	23.81	5	SNV
AIDTg	(+)	T	Olfr1414	1	94408419	30	A	G	20	6	SNV
AIDTg	(+)	T	Hdlbp	1	95326808	18	T	A	22.22	4	SNV
AIDTg	(+)	T	Cdh20	1	106850655	17	A	G	23.53	4	SNV
AIDTg	(+)	T	Serpinb3a	1	108942922	24	A	G	20.83	5	SNV
AIDTg	(+)	T	Dbi	1	122017429	41	G	A	17.07	7	SNV
AIDTg	(+)	T	Ppp1r12b	1	136769474	22	T	G	18.18	4	SNV
AIDTg	(+)	T	Nek7	1	140383596	26	G	A	23.08	6	SNV
AIDTg	(+)	T	Nek7	1	140383597	27	C	T	18.52	5	SNV
AIDTg	(+)	T	Olfml2b	1	172599212	32	T	C	15.62	5	SNV
AIDTg	(+)	T	Apoa2	1	173156352	31	C	T	19.35	6	SNV
AIDTg	(+)	T	Ly9	1	173524015	30	C	A	20	6	SNV
AIDTg	(+)	T	Olfr218	1	175134127	32	T	A	15.62	5	SNV
AIDTg	(+)	T	Olfr433	1	175972102	38	C	G	21.05	8	SNV
AIDTg	(+)	T	G0s2	1	195098872	50	G	T	18	9	SNV
AIDTg	(+)	T	Suv39h2	2	3381630	21	C	A	23.81	5	SNV
AIDTg	(+)	T	Cubn	2	13310573	20	T	C	20	4	SNV
AIDTg	(+)	T	Cubn	2	13310574	19	G	Del	21.05	4	indel
AIDTg	(+)	T	Cubn	2	13310575	19	T	Del	21.05	4	indel
AIDTg	(+)	T	BC061194	2	18653592	20	G	T	25	5	SNV
AIDTg	(+)	T	Ubac1	2	25860962	17	C	T	23.53	4	SNV

AIDTg	(+)	T	Notch1	2	26327742	18	C	Del	22.22	4	indel
AIDTg	(+)	T	Gbgt1	2	28353904	19	T	Del	21.05	4	indel
AIDTg	(+)	T	Dpm2	2	32426738	22	G	T	22.73	5	SNV
AIDTg	(+)	T	Gapvd1	2	34534141	22	G	A	18.18	4	SNV
AIDTg	(+)	T	Rbm18	2	35989719	25	A	C	20	5	SNV
AIDTg	(+)	T	Rc3h2	2	37237424	24	G	A	16.67	4	SNV
AIDTg	(+)	T	Ttn	2	76714584	23	C	A	26.09	6	SNV
AIDTg	(+)	T	Itga4	2	79132286	17	C	A	29.41	5	SNV
AIDTg	(+)	T	Zdhhc5	2	84531375	20	C	G	25	5	SNV
AIDTg	(+)	T	Zdhhc5	2	84531376	20	C	T	25	5	SNV
AIDTg	(+)	T	Slc43a1	2	84703107	27	G	Del	18.52	5	indel
AIDTg	(+)	T	Slc43a1	2	84703108	27	G	Del	18.52	5	indel
AIDTg	(+)	T	Olfr1023	2	85727479	36	T	C	22.22	8	SNV
AIDTg	(+)	T	Olfr1122	2	87228390	21	T	C	19.05	4	SNV
AIDTg	(+)	T	Olfr1158	2	87830542	28	G	T	21.43	6	SNV
AIDTg	(+)	T	Olfr1168	2	88025749	38	C	A	15.79	6	SNV
AIDTg	(+)	T	Olfr1189	2	88432467	22	T	A	18.18	4	SNV
AIDTg	(+)	T	Olfr1265	2	89877578	33	T	A	15.15	5	SNV
AIDTg	(+)	T	Olfr1269	2	89959255	20	A	T	20	4	SNV
AIDTg	(+)	T	Olfr1272	2	90122103	21	A	C	28.57	6	SNV
AIDTg	(+)	T	Phf21a	2	92168519	26	T	G	15.38	4	SNV
AIDTg	(+)	T	Ttc17	2	94182856	21	G	T	19.05	4	SNV
AIDTg	(+)	T	Hipk3	2	104270155	40	T	A	15	6	SNV
AIDTg	(+)	T	Tmco5b	2	113137119	36	T	G	16.67	6	SNV
AIDTg	(+)	T	Aqr	2	113933912	24	T	A	16.67	4	SNV
AIDTg	(+)	T	Duox1	2	122141439	22	A	T	18.18	4	SNV
AIDTg	(+)	T	Duox1	2	122141444	23	G	Del	17.39	4	indel
AIDTg	(+)	T	F830045P16Rik	2	129298603	37	T	Del	16.22	6	indel
AIDTg	(+)	T	Plcb4	2	135777798	25	A	C	20	5	SNV
AIDTg	(+)	T	RP23-244H7.9	2	153753070	18	C	A	22.22	4	SNV
AIDTg	(+)	T	RP23-244H7.9	2	153753071	18	C	A	22.22	4	SNV
AIDTg	(+)	T	Lpin3	2	160722518	19	G	T	21.05	4	SNV
AIDTg	(+)	T	Sycp2	2	178091317	24	T	G	29.17	7	SNV
AIDTg	(+)	T	Lama5	2	179918152	26	C	A	15.38	4	SNV
AIDTg	(+)	T	Zfhx4	3	5412792	33	C	T	15.15	5	SNV

AIDTg	(+)	T	Pld1	3	28008712	20	G	A	20	4	SNV
AIDTg	(+)	T	Exosc9	3	36454410	21	C	G	19.05	4	SNV
AIDTg	(+)	T	Slc7a11	3	50184969	23	T	Del	21.74	5	indel
AIDTg	(+)	T	Slc7a11	3	50184970	23	C	Del	21.74	5	indel
AIDTg	(+)	T	Trpc4	3	54070314	20	G	A	20	4	SNV
AIDTg	(+)	T	Trpc4	3	54070315	20	G	C	20	4	SNV
AIDTg	(+)	T	1110032A04Rik	3	69624959	24	G	T	20.83	5	SNV
AIDTg	(+)	T	Sis	3	72742673	22	T	Ins	22.73	5	indel
AIDTg	(+)	T	Pet112l	3	85409044	30	C	A	16.67	5	SNV
AIDTg	(+)	T	Lrba	3	86585493	22	G	T	18.18	4	SNV
AIDTg	(+)	T	Fdps	3	88898851	22	G	Del	18.18	4	indel
AIDTg	(+)	T	Fdps	3	88898852	23	T	Del	17.39	4	indel
AIDTg	(+)	T	Hist2h2ac	3	96024419	156	G	A	22.44	35	SNV
AIDTg	(+)	T	Rnf115	3	96561906	23	A	T	17.39	4	SNV
AIDTg	(+)	T	Trim33	3	103148547	24	A	G	16.67	4	SNV
AIDTg	(+)	T	Phtf1	3	103789810	26	A	G	15.38	4	SNV
AIDTg	(+)	T	Adora3	3	105710690	18	C	G	22.22	4	SNV
AIDTg	(+)	T	Chi3l3	3	105963318	36	T	A	16.67	6	SNV
AIDTg	(+)	T	Wdr47	3	108447495	21	T	G	19.05	4	SNV
AIDTg	(+)	T	Frrs1	3	116581358	21	C	T	19.05	4	SNV
AIDTg	(+)	T	Clca3	3	144695635	18	G	C	22.22	4	SNV
AIDTg	(+)	T	Clca3	3	144695636	18	A	T	22.22	4	SNV
AIDTg	(+)	T	Slc7a13	4	19768576	27	C	G	22.22	6	SNV
AIDTg	(+)	T	Ube2r2	4	41137748	16	C	A	25	4	SNV
AIDTg	(+)	T	Unc13b	4	43108650	26	T	G	19.23	5	SNV
AIDTg	(+)	T	Unc13b	4	43253999	20	A	T	25	5	SNV
AIDTg	(+)	T	Creb3	4	43578992	23	G	T	17.39	4	SNV
AIDTg	(+)	T	Olfr159	4	43783774	32	G	A	15.62	5	SNV
AIDTg	(+)	T	Anp32b	4	46485012	25	G	T	24	6	SNV
AIDTg	(+)	T	Anks6	4	47038596	21	A	Del	19.05	4	indel
AIDTg	(+)	T	Anks6	4	47038597	21	T	Del	19.05	4	indel
AIDTg	(+)	T	Anks6	4	47038598	21	A	Del	19.05	4	indel
AIDTg	(+)	T	Anks6	4	47038599	21	A	Del	19.05	4	indel
AIDTg	(+)	T	Tex10	4	48464881	22	G	C	22.73	5	SNV
AIDTg	(+)	T	Rnf20	4	49661317	35	C	T	17.14	6	SNV

AIDTg	(+)	T	Cdc26	4	62063800	18	G	T	22.22	4	SNV
AIDTg	(+)	T	Cdk5rap2	4	69928019	18	T	G	22.22	4	SNV
AIDTg	(+)	T	Cdk5rap2	4	69942332	20	T	C	20	4	SNV
AIDTg	(+)	T	Cdk5rap2	4	69978618	22	T	C	27.27	6	SNV
AIDTg	(+)	T	Mpdz	4	80963597	24	C	T	16.67	4	SNV
AIDTg	(+)	T	Cer1	4	82530783	32	C	T	25	8	SNV
AIDTg	(+)	T	Jun	4	94717752	56	G	A	17.86	10	SNV
AIDTg	(+)	T	Cyp2j11	4	95983094	16	T	G	25	4	SNV
AIDTg	(+)	T	Dhcr24	4	106233976	112	C	T	19.64	22	SNV
AIDTg	(+)	T	Nrd1	4	108686375	53	A	T	20.75	11	SNV
AIDTg	(+)	T	Cyp4x1	4	114785537	18	G	T	22.22	4	SNV
AIDTg	(+)	T	Urod	4	116662896	39	T	C	17.95	7	SNV
AIDTg	(+)	T	Urod	4	116662898	38	C	G	18.42	7	SNV
AIDTg	(+)	T	Plk3	4	116806039	59	G	A	18.64	11	SNV
AIDTg	(+)	T	Plk3	4	116806090	25	G	A	16	4	SNV
AIDTg	(+)	T	Kdm4a	4	117821420	37	C	A	16.22	6	SNV
AIDTg	(+)	T	Olfr1338	4	118426456	23	A	G	17.39	4	SNV
AIDTg	(+)	T	4930538K18Rik	4	118883524	47	G	T	19.15	9	SNV
AIDTg	(+)	T	4930538K18Rik	4	118883526	39	A	T	17.95	7	SNV
AIDTg	(+)	T	Csf3r	4	125712570	22	G	T	22.73	5	SNV
AIDTg	(+)	T	Pum1	4	130330405	34	C	T	17.65	6	SNV
AIDTg	(+)	T	Pum1	4	130330409	34	G	Del	17.65	6	indel
AIDTg	(+)	T	Pum1	4	130330410	38	G	Del	15.79	6	indel
AIDTg	(+)	T	Epb4.1	4	131513707	17	T	Del	23.53	4	indel
AIDTg	(+)	T	Nr0b2	4	133109637	52	C	T	15.38	8	SNV
AIDTg	(+)	T	Id3	4	135700218	23	C	T	17.39	4	SNV
AIDTg	(+)	T	Id3	4	135700220	23	C	T	17.39	4	SNV
AIDTg	(+)	T	Dnajc16	4	141319726	24	G	T	25	6	SNV
AIDTg	(+)	T	Dnajc16	4	141319727	24	C	G	25	6	SNV
AIDTg	(+)	T	Kcnab2	4	151769330	29	A	C	17.24	5	SNV
AIDTg	(+)	T	Paxip1	5	28083514	50	C	Del	16	8	indel
AIDTg	(+)	T	Htr5a	5	28169028	23	A	C	17.39	4	SNV
AIDTg	(+)	T	Insig1	5	28398260	44	C	T	15.91	7	SNV
AIDTg	(+)	T	Prom1	5	44425639	23	G	C	21.74	5	SNV
AIDTg	(+)	T	Gabra2	5	71353235	16	A	G	25	4	SNV

AIDTg	(+)	T	Aasdh	5	77325440	24	C	A	16.67	4	SNV
AIDTg	(+)	T	Fras1	5	96983886	25	C	A	20	5	SNV
AIDTg	(+)	T	Pgam5	5	110696214	31	T	A	16.13	5	SNV
AIDTg	(+)	T	Hip1r	5	124450221	30	A	C	16.67	5	SNV
AIDTg	(+)	T	Stx2	5	129494724	33	T	C	27.27	9	SNV
AIDTg	(+)	T	Ywhag	5	136410255	37	G	A	18.92	7	SNV
AIDTg	(+)	T	Trip6	5	137751915	48	T	G	18.75	9	SNV
AIDTg	(+)	T	Lmtk2	5	144909149	18	T	C	22.22	4	SNV
AIDTg	(+)	T	Hepacam2	6	3436924	20	A	T	20	4	SNV
AIDTg	(+)	T	Cav1	6	17289214	18	T	C	22.22	4	SNV
AIDTg	(+)	T	Ptprz1	6	22950243	22	T	C	18.18	4	SNV
AIDTg	(+)	T	Grm8	6	27235873	19	G	T	26.32	5	SNV
AIDTg	(+)	T	Flnc	6	29411188	22	C	A	18.18	4	SNV
AIDTg	(+)	T	Moxd2	6	40835440	25	G	T	16	4	SNV
AIDTg	(+)	T	Eapa2	6	42541298	18	C	Del	22.22	4	indel
AIDTg	(+)	T	Olfr47	6	43186115	41	A	C	17.07	7	SNV
AIDTg	(+)	T	Olfr47	6	43186116	41	C	A	17.07	7	SNV
AIDTg	(+)	T	4921507P07Rik	6	50534469	21	A	T	23.81	5	SNV
AIDTg	(+)	T	Abcg2	6	58619185	24	T	A	25	6	SNV
AIDTg	(+)	T	Cd8a	6	71323691	29	G	T	17.24	5	SNV
AIDTg	(+)	T	Polr1a	6	71899460	30	A	C	23.33	7	SNV
AIDTg	(+)	T	Elmod3	6	72530348	22	A	Del	18.18	4	indel
AIDTg	(+)	T	Dguok	6	83431424	61	T	Del	16.39	10	indel
AIDTg	(+)	T	Pcbp1	6	86475224	53	G	A	18.87	10	SNV
AIDTg	(+)	T	Copg	6	87840258	20	A	T	20	4	SNV
AIDTg	(+)	T	Klf15	6	90416454	28	C	T	21.43	6	SNV
AIDTg	(+)	T	Klf15	6	90416582	59	C	T	16.95	10	SNV
AIDTg	(+)	T	Bhlhe40	6	108610969	32	G	A	18.75	6	SNV
AIDTg	(+)	T	Slc6a1	6	114261849	25	G	A	16	4	SNV
AIDTg	(+)	T	Clec4b1	6	123019725	20	T	A	20	4	SNV
AIDTg	(+)	T	Lpcat3	6	124648150	33	C	A	15.15	5	SNV
AIDTg	(+)	T	Lpcat3	6	124648151	33	T	C	15.15	5	SNV
AIDTg	(+)	T	Nrip2	6	128356536	32	T	G	15.62	5	SNV
AIDTg	(+)	T	BC048546	6	128516345	28	C	T	25	7	SNV
AIDTg	(+)	T	Clec2h	6	128625862	17	G	A	23.53	4	SNV

AIDTg	(+)	T	St8sia1	6	142862641	24	G	A	16.67	4	SNV
AIDTg	(+)	T	Itpr2	6	146345553	25	G	T	16	4	SNV
AIDTg	(+)	T	Itpr2	6	146345554	25	T	C	16	4	SNV
AIDTg	(+)	T	Pira3	7	3866495	20	G	A	20	4	SNV
AIDTg	(+)	T	V1rd10	7	5405916	18	C	G	22.22	4	SNV
AIDTg	(+)	T	Slc27a5	7	13580341	26	C	Del	15.38	4	indel
AIDTg	(+)	T	Slc27a5	7	13580342	26	A	Del	15.38	4	indel
AIDTg	(+)	T	Slc27a5	7	13580343	26	C	Del	15.38	4	indel
AIDTg	(+)	T	Psg18	7	18934606	21	G	Del	19.05	4	indel
AIDTg	(+)	T	Psg21	7	19240202	25	G	T	16	4	SNV
AIDTg	(+)	T	Psg17	7	19399990	18	C	G	22.22	4	SNV
AIDTg	(+)	T	Apoe	7	20281847	58	C	T	15.52	9	SNV
AIDTg	(+)	T	Apoe	7	20282392	30	C	T	16.67	5	SNV
AIDTg	(+)	T	V1rd7	7	24418221	20	G	T	25	5	SNV
AIDTg	(+)	T	Grik5	7	25808393	29	G	C	17.24	5	SNV
AIDTg	(+)	T	Ryr1	7	29851616	21	T	A	19.05	4	SNV
AIDTg	(+)	T	Cebpa	7	35905385	37	G	A	18.92	7	SNV
AIDTg	(+)	T	Cebpa	7	35905430	29	G	C	17.24	5	SNV
AIDTg	(+)	T	Ceacam18	7	50897441	17	T	A	29.41	5	SNV
AIDTg	(+)	T	Gabrb3	7	65071669	15	C	G	26.67	4	SNV
AIDTg	(+)	T	Blm	7	87647460	24	T	A	16.67	4	SNV
AIDTg	(+)	T	Olfr304	7	93535067	23	T	A	21.74	5	SNV
AIDTg	(+)	T	Thrsp	7	104565611	20	C	T	20	4	SNV
AIDTg	(+)	T	Olfr556	7	109818652	30	G	C	23.33	7	SNV
AIDTg	(+)	T	Olfr556	7	109818655	27	G	T	18.52	5	SNV
AIDTg	(+)	T	Olfr633	7	111095898	26	C	G	19.23	5	SNV
AIDTg	(+)	T	Olfr704	7	114008694	20	T	G	20	4	SNV
AIDTg	(+)	T	Olfr704	7	114008697	21	C	A	19.05	4	SNV
AIDTg	(+)	T	Olfr470	7	114988649	46	T	A	28.26	13	SNV
AIDTg	(+)	T	Gde1	7	125842199	25	T	Del	16	4	indel
AIDTg	(+)	T	Gtf3c1	7	132790223	20	A	T	20	4	SNV
AIDTg	(+)	T	Nupr1	7	133768848	55	T	A	21.82	12	SNV
AIDTg	(+)	T	Sephs2	7	134416238	29	C	T	17.24	5	SNV
AIDTg	(+)	T	Phkg2	7	134721532	24	G	C	16.67	4	SNV
AIDTg	(+)	T	Bnip3	7	146089713	38	T	G	15.79	6	SNV

AIDTg	(+)	T	Bnip3	7	146089743	27	G	T	29.63	8	SNV
AIDTg	(+)	T	Olfr535	7	147679005	20	T	A	20	4	SNV
AIDTg	(+)	T	Olfr535	7	147679006	20	A	C	20	4	SNV
AIDTg	(+)	T	Olfr536	7	147690041	22	C	T	22.73	5	SNV
AIDTg	(+)	T	Athl1	7	148130631	23	G	T	17.39	4	SNV
AIDTg	(+)	T	Muc5ac	7	148974974	44	G	C	15.91	7	SNV
AIDTg	(+)	T	6330512M04Rik	7	149514514	26	T	Del	23.08	6	indel
AIDTg	(+)	T	6330512M04Rik	7	149514515	25	G	Del	24	6	indel
AIDTg	(+)	T	6330512M04Rik	7	149514519	21	C	T	19.05	4	SNV
AIDTg	(+)	T	Ankrd10	8	11619226	19	A	G	21.05	4	SNV
AIDTg	(+)	T	Ido1	8	25697407	25	C	A	20	5	SNV
AIDTg	(+)	T	Pdlim3	8	46993914	22	C	G	27.27	6	SNV
AIDTg	(+)	T	Zfp869	8	72232252	23	T	A	21.74	5	SNV
AIDTg	(+)	T	Zfp869	8	72232253	23	T	C	21.74	5	SNV
AIDTg	(+)	T	Gatad2a	8	72441677	23	A	C	17.39	4	SNV
AIDTg	(+)	T	Ddx49	8	72821193	28	G	C	17.86	5	SNV
AIDTg	(+)	T	Large	8	75347727	23	A	T	17.39	4	SNV
AIDTg	(+)	T	Mcm5	8	77648707	23	G	A	17.39	4	SNV
AIDTg	(+)	T	Zfp330	8	85288792	19	C	T	21.05	4	SNV
AIDTg	(+)	T	Zfp330	8	85288793	19	C	T	21.05	4	SNV
AIDTg	(+)	T	2310036O22Rik	8	87551037	26	A	C	19.23	5	SNV
AIDTg	(+)	T	Mylk3	8	87883128	26	T	Del	19.23	5	indel
AIDTg	(+)	T	Mylk3	8	87883130	26	C	A	19.23	5	SNV
AIDTg	(+)	T	Tmco7	8	109305660	15	G	T	26.67	4	SNV
AIDTg	(+)	T	Hp	8	112099187	35	G	C	17.14	6	SNV
AIDTg	(+)	T	Taf1c	8	122128172	24	T	G	16.67	4	SNV
AIDTg	(+)	T	Pard3	8	129894180	17	A	C	23.53	4	SNV
AIDTg	(+)	T	8430410K20Rik	9	4383997	26	C	T	15.38	4	SNV
AIDTg	(+)	T	8430410K20Rik	9	4383998	26	T	C	15.38	4	SNV
AIDTg	(+)	T	Cypt4	9	24429794	23	C	T	17.39	4	SNV
AIDTg	(+)	T	Olfr885	9	37869389	32	C	G	25	8	SNV
AIDTg	(+)	T	Olfr143	9	38061522	31	T	G	16.13	5	SNV
AIDTg	(+)	T	Olfr143	9	38061523	31	T	A	16.13	5	SNV
AIDTg	(+)	T	Olfr901	9	38238275	47	T	G	17.02	8	SNV
AIDTg	(+)	T	Olfr914	9	38414453	22	T	A	18.18	4	SNV

AIDTg	(+)	T	Olfr965	9	39527281	26	C	Del	23.08	6	indel
AIDTg	(+)	T	Olfr969	9	39603055	25	C	A	16	4	SNV
AIDTg	(+)	T	Olfr970	9	39627905	23	G	T	17.39	4	SNV
AIDTg	(+)	T	Olfr970	9	39627909	22	T	G	18.18	4	SNV
AIDTg	(+)	T	Cbl	9	44009232	22	A	G	18.18	4	SNV
AIDTg	(+)	T	Apoa1	9	46037046	41	G	A	19.51	8	SNV
AIDTg	(+)	T	Cib2	9	54393711	18	G	C	22.22	4	SNV
AIDTg	(+)	T	Ccdc33	9	57906100	23	A	Del	21.74	5	indel
AIDTg	(+)	T	Lrrc49	9	60469496	26	C	A	15.38	4	SNV
AIDTg	(+)	T	Ccnb2	9	70266819	16	G	C	25	4	SNV
AIDTg	(+)	T	Prtg	9	72690503	20	T	C	20	4	SNV
AIDTg	(+)	T	Morf4l1	9	89992213	17	T	G	23.53	4	SNV
AIDTg	(+)	T	Amt	9	108201223	23	T	Del	17.39	4	indel
AIDTg	(+)	T	Slc6a20b	9	123514004	38	C	T	15.79	6	SNV
AIDTg	(+)	T	Cnksr3	10	3219789	18	C	A	22.22	4	SNV
AIDTg	(+)	T	Plekhg1	10	6382325	23	A	C	17.39	4	SNV
AIDTg	(+)	T	Utrn	10	12159584	20	T	G	25	5	SNV
AIDTg	(+)	T	Taar7d	10	23747535	39	T	A	15.38	6	SNV
AIDTg	(+)	T	Dse	10	33872324	29	C	G	17.24	5	SNV
AIDTg	(+)	T	Nt5dc1	10	34034664	30	T	C	16.67	5	SNV
AIDTg	(+)	T	Gprc6a	10	51334880	30	C	A	23.33	7	SNV
AIDTg	(+)	T	Gprc6a	10	51334881	31	A	T	22.58	7	SNV
AIDTg	(+)	T	LOC100504180	10	57687424	47	G	A	19.15	9	SNV
AIDTg	(+)	T	Supv3l1	10	61906268	19	A	T	21.05	4	SNV
AIDTg	(+)	T	Herc4	10	62741108	18	C	G	27.78	5	SNV
AIDTg	(+)	T	Lss	10	76001152	16	T	G	25	4	SNV
AIDTg	(+)	T	Trappc10	10	77663378	25	G	T	16	4	SNV
AIDTg	(+)	T	Gnptab	10	87863412	20	A	G	20	4	SNV
AIDTg	(+)	T	Dusp6	10	98726454	39	G	A	15.38	6	SNV
AIDTg	(+)	T	Syt1	10	108079346	37	T	C	16.22	6	SNV
AIDTg	(+)	T	Syt1	10	108079347	37	T	A	16.22	6	SNV
AIDTg	(+)	T	Frs2	10	116514591	21	G	T	28.57	6	SNV
AIDTg	(+)	T	Cs	10	127797114	25	C	A	20	5	SNV
AIDTg	(+)	T	Obfc2b	10	127845847	23	T	G	17.39	4	SNV
AIDTg	(+)	T	Si	10	128151418	26	T	C	23.08	6	SNV

AIDTg	(+)	T	Si	10	128151421	21	C	T	28.57	6	SNV
AIDTg	(+)	T	Olfr800	10	129097425	30	G	C	20	6	SNV
AIDTg	(+)	T	Olfr800	10	129097427	31	A	C	19.35	6	SNV
AIDTg	(+)	T	Sec14l2	11	4003527	27	A	C	18.52	5	SNV
AIDTg	(+)	T	Sf3a1	11	4076379	26	G	C	19.23	5	SNV
AIDTg	(+)	T	Znrf3	11	5189696	30	A	T	26.67	8	SNV
AIDTg	(+)	T	Igfbp1	11	7098022	86	G	A	15.12	13	SNV
AIDTg	(+)	T	Igfbp1	11	7098031	90	G	T	16.67	15	SNV
AIDTg	(+)	T	Igfbp1	11	7098147	37	C	T	16.22	6	SNV
AIDTg	(+)	T	Abca13	11	9470662	26	G	A	23.08	6	SNV
AIDTg	(+)	T	Sgcd	11	46896332	25	G	A	20	5	SNV
AIDTg	(+)	T	Sgcd	11	46896333	25	G	T	20	5	SNV
AIDTg	(+)	T	Olfr1392	11	49106920	17	G	C	23.53	4	SNV
AIDTg	(+)	T	Olfr10	11	49131676	32	T	G	28.12	9	SNV
AIDTg	(+)	T	Olfr1381	11	49365508	42	T	A	23.81	10	SNV
AIDTg	(+)	T	Olfr1377	11	50798802	25	T	C	16	4	SNV
AIDTg	(+)	T	Olfr1371	11	52027335	90	T	Del	17.78	16	indel
AIDTg	(+)	T	Olfr1371	11	52027336	81	C	Del	19.75	16	indel
AIDTg	(+)	T	Gdf9	11	53250192	37	T	A	16.22	6	SNV
AIDTg	(+)	T	Flcn	11	59606290	24	A	T	20.83	5	SNV
AIDTg	(+)	T	Cxcl16	11	70269347	22	A	C	18.18	4	SNV
AIDTg	(+)	T	Abr	11	76292668	40	C	Del	15	6	indel
AIDTg	(+)	T	Abr	11	76292669	40	A	Del	15	6	indel
AIDTg	(+)	T	4932411E22Rik	11	89266807	23	C	A	17.39	4	SNV
AIDTg	(+)	T	Cdc6	11	98773505	27	A	T	18.52	5	SNV
AIDTg	(+)	T	Ubtf	11	102167990	26	A	Del	15.38	4	indel
AIDTg	(+)	T	Prkca	11	107842956	25	G	A	16	4	SNV
AIDTg	(+)	T	Dnaic2	11	114615637	21	A	T	19.05	4	SNV
AIDTg	(+)	T	Slc9a3r1	11	115024942	46	G	A	19.57	9	SNV
AIDTg	(+)	T	Slc9a3r1	11	115024950	56	G	A	17.86	10	SNV
AIDTg	(+)	T	Slc9a3r1	11	115025111	40	T	Del	15	6	indel
AIDTg	(+)	T	Slc9a3r1	11	115025112	38	C	Del	15.79	6	indel
AIDTg	(+)	T	Rhob	12	8505963	24	C	T	16.67	4	SNV
AIDTg	(+)	T	Id2	12	25780721	18	C	T	27.78	5	SNV
AIDTg	(+)	T	Nin	12	71126429	30	T	A	16.67	5	SNV

AIDTg	(+)	T	Fntb	12	77998386	18	C	T	22.22	4	SNV
AIDTg	(+)	T	Slc8a3	12	82305110	21	T	A	28.57	6	SNV
AIDTg	(+)	T	Acot2	12	85328932	26	A	C	15.38	4	SNV
AIDTg	(+)	T	Wdr20a	12	112031973	23	G	A	21.74	5	SNV
AIDTg	(+)	T	Wdr20a	12	112032370	22	T	G	18.18	4	SNV
AIDTg	(+)	T	Psma2	13	14711666	21	G	C	28.57	6	SNV
AIDTg	(+)	T	Olfr263-ps1	13	21225198	44	G	A	22.73	10	SNV
AIDTg	(+)	T	Olfr263-ps1	13	21225200	45	C	A	22.22	10	SNV
AIDTg	(+)	T	Hist1h2ak	13	21845418	33	C	G	18.18	6	SNV
AIDTg	(+)	T	Hist1h2ak	13	21845442	26	C	T	19.23	5	SNV
AIDTg	(+)	T	Hist1h4d	13	23673485	56	G	A	17.86	10	SNV
AIDTg	(+)	T	Hist1h1e	13	23713917	22	G	A	18.18	4	SNV
AIDTg	(+)	T	Hist1h3c	13	23836961	21	C	A	28.57	6	SNV
AIDTg	(+)	T	E2f3	13	30005284	26	C	Del	15.38	4	indel
AIDTg	(+)	T	E2f3	13	30005285	26	A	Del	15.38	4	indel
AIDTg	(+)	T	Bmp6	13	38590799	17	G	C	23.53	4	SNV
AIDTg	(+)	T	Dapk1	13	60829876	23	T	A	17.39	4	SNV
AIDTg	(+)	T	BC051665	13	60886501	45	A	T	22.22	10	SNV
AIDTg	(+)	T	Mctp1	13	77164056	21	G	Del	19.05	4	indel
AIDTg	(+)	T	Polr3g	13	81833741	18	T	C	22.22	4	SNV
AIDTg	(+)	T	Vcan	13	89845293	29	T	A	20.69	6	SNV
AIDTg	(+)	T	Serinc5	13	93476225	43	G	Del	16.28	7	indel
AIDTg	(+)	T	Serinc5	13	93476226	43	A	Del	16.28	7	indel
AIDTg	(+)	T	Serinc5	13	93476227	43	C	T	18.6	8	SNV
AIDTg	(+)	T	Bhmt	13	94390078	22	T	Del	22.73	5	indel
AIDTg	(+)	T	Kif2a	13	107783330	28	G	Del	17.86	5	indel
AIDTg	(+)	T	Itga1	13	115820369	20	A	Del	20	4	indel
AIDTg	(+)	T	Camk2g	14	21584173	26	G	C	19.23	5	SNV
AIDTg	(+)	T	Ptpn20	14	34446215	18	C	A	22.22	4	SNV
AIDTg	(+)	T	Ptpn20	14	34446216	18	C	A	22.22	4	SNV
AIDTg	(+)	T	Ddhd1	14	46215337	22	C	T	27.27	6	SNV
AIDTg	(+)	T	Olfr1508	14	53083280	19	A	G	26.32	5	SNV
AIDTg	(+)	T	Nfatc4	14	56452428	45	C	T	17.78	8	SNV
AIDTg	(+)	T	Loxl2	14	70044564	22	C	A	18.18	4	SNV
AIDTg	(+)	T	Zc3h13	14	75721482	21	T	A	23.81	5	SNV

AIDTg	(+)	T	Trps1	15	50492766	20	G	C	25	5	SNV
AIDTg	(+)	T	Trps1	15	50492767	20	T	C	25	5	SNV
AIDTg	(+)	T	Pim3	15	88695015	59	G	A	15.25	9	SNV
AIDTg	(+)	T	Dip2b	15	100003724	27	T	A	22.22	6	SNV
AIDTg	(+)	T	Dnaja3	16	4697276	30	G	C	26.67	8	SNV
AIDTg	(+)	T	Crkl	16	17483858	19	T	Del	21.05	4	indel
AIDTg	(+)	T	Rtn4r	16	18151449	53	G	C	15.09	8	SNV
AIDTg	(+)	T	Ece2	16	20617818	23	A	T	17.39	4	SNV
AIDTg	(+)	T	Gm606	16	26960619	21	G	A	23.81	5	SNV
AIDTg	(+)	T	Itgb5	16	33899342	33	C	G	18.18	6	SNV
AIDTg	(+)	T	Polq	16	37065482	24	G	Del	20.83	5	indel
AIDTg	(+)	T	4932425I24Rik	16	38320424	28	T	Del	17.86	5	indel
AIDTg	(+)	T	Cd96	16	46036075	36	A	G	16.67	6	SNV
AIDTg	(+)	T	Cd96	16	46036077	36	G	T	16.67	6	SNV
AIDTg	(+)	T	Gart	16	91639611	25	A	T	16	4	SNV
AIDTg	(+)	T	Cryzl1	16	91699483	28	A	Del	25	7	indel
AIDTg	(+)	T	Cryzl1	16	91699484	28	A	Del	25	7	indel
AIDTg	(+)	T	Atp5o	16	91925548	20	C	A	20	4	SNV
AIDTg	(+)	T	Atp5o	16	91925549	23	T	A	17.39	4	SNV
AIDTg	(+)	T	Atp5o	16	91925829	25	T	A	16	4	SNV
AIDTg	(+)	T	Itgb2l	16	96647829	29	G	A	20.69	6	SNV
AIDTg	(+)	T	Acat3	17	13119353	27	T	A	25.93	7	SNV
AIDTg	(+)	T	D17Wsu92e	17	27957149	28	C	T	21.43	6	SNV
AIDTg	(+)	T	Mapk13	17	28912227	19	G	T	21.05	4	SNV
AIDTg	(+)	T	Dnahc8	17	30892113	36	G	T	16.67	6	SNV
AIDTg	(+)	T	H2-Eb2	17	34470414	24	T	G	20.83	5	SNV
AIDTg	(+)	T	C4b	17	34875940	18	A	C	22.22	4	SNV
AIDTg	(+)	T	H2-Q10	17	35607943	80	G	A	16.25	13	SNV
AIDTg	(+)	T	H2-M10.3	17	36504948	16	C	A	25	4	SNV
AIDTg	(+)	T	Olfr96	17	37362963	17	G	A	23.53	4	SNV
AIDTg	(+)	T	Olfr121	17	37889184	24	C	T	20.83	5	SNV
AIDTg	(+)	T	Supt3h	17	45140085	25	T	C	24	6	SNV
AIDTg	(+)	T	Med20	17	47759988	18	A	G	22.22	4	SNV
AIDTg	(+)	T	Ptprm	17	67047775	18	G	C	22.22	4	SNV
AIDTg	(+)	T	Tgif1	17	71195532	26	T	C	15.38	4	SNV

AIDTg	(+)	T	Alk	17	72250654	16	G	C	25	4	SNV
AIDTg	(+)	T	Galnt14	17	73894432	23	G	Del	21.74	5	indel
AIDTg	(+)	T	Heatr5b	17	79156325	21	T	A	19.05	4	SNV
AIDTg	(+)	T	Eif2ak2	17	79257890	26	T	G	19.23	5	SNV
AIDTg	(+)	T	Eif2ak2	17	79257891	26	T	Del	19.23	5	indel
AIDTg	(+)	T	Eif2ak2	17	79257892	26	T	Del	19.23	5	indel
AIDTg	(+)	T	Npc1	18	12369028	23	G	C	17.39	4	SNV
AIDTg	(+)	T	Ttc39c	18	12802535	26	G	A	15.38	4	SNV
AIDTg	(+)	T	Ss18	18	14809736	25	T	C	24	6	SNV
AIDTg	(+)	T	Dsg4	18	20625095	26	C	A	15.38	4	SNV
AIDTg	(+)	T	Kdm3b	18	34973123	52	C	G	15.38	8	SNV
AIDTg	(+)	T	Egr1	18	35021256	39	G	A	17.95	7	SNV
AIDTg	(+)	T	Egr1	18	35022212	61	C	A	18.03	11	SNV
AIDTg	(+)	T	Fbxo38	18	62676683	21	C	A	19.05	4	SNV
AIDTg	(+)	T	Fbxo38	18	62676684	21	C	G	19.05	4	SNV
AIDTg	(+)	T	Sf3b2	19	5287547	16	T	A	25	4	SNV
AIDTg	(+)	T	Slc22a12	19	6540587	21	T	G	19.05	4	SNV
AIDTg	(+)	T	Ms4a6b	19	11596214	82	A	G	17.07	14	SNV
AIDTg	(+)	T	Olfr1417	19	11902788	43	A	T	20.93	9	SNV
AIDTg	(+)	T	Olfr1450	19	13028189	31	A	G	19.35	6	SNV
AIDTg	(+)	T	Olfr1474	19	13545795	22	A	G	18.18	4	SNV
AIDTg	(+)	T	Olfr1474	19	13545797	21	C	A	19.05	4	SNV
AIDTg	(+)	T	Olfr1474	19	13545919	79	A	T	15.19	12	SNV
AIDTg	(+)	T	Olfr1484	19	13659957	28	C	G	21.43	6	SNV
AIDTg	(+)	T	Smarca2	19	26738592	24	G	T	16.67	4	SNV
AIDTg	(+)	T	Ak3	19	29100783	20	C	T	20	4	SNV
AIDTg	(+)	T	Rbp4	19	38198810	31	G	A	16.13	5	SNV
AIDTg	(+)	T	Cyp2c65	19	39143981	26	A	T	19.23	5	SNV
AIDTg	(+)	T	Cyp2c65	19	39143982	25	G	A	20	5	SNV
AIDTg	(+)	T	Dclre1a	19	56618826	17	T	G	23.53	4	SNV
AIDTg	(+)	T	Hcfc1	X	71198700	21	A	G	19.05	4	SNV
AIDTg	(+)	T	Tsc22d3	X	137132718	29	C	T	20.69	6	SNV

* T: tumor, NT: nontumor

** Chr: chromosome

*** SNV: single nucleotide variants, indel: insertion or deletion mutation

Supplementary Table 6. Genes upregulated by TAA in both WT and AID Tg mice.

Gene symbol	Gene ID	Fold change in WT mice	Fold change in AID Tg mice
1200009I06Rik	NM_028807	2.57	2.07
1700047I17Rik2	NM_001100116	2.16	2.34
2010002N04Rik	NM_134133	5.03	3.97
2410089E03Rik	NM_001162906	2.55	2.46
4930417M19Rik	NM_177195	6.60	3.40
4930513E20Rik	AK019679	2.22	2.02
5330421C15Rik	AK039175	3.69	6.16
5730409E04Rik	NM_001145950	3.35	3.45
9030619P08Rik	NM_001039720	7.49	2.23
A_55_P1953377	A_55_P1953377	2.95	2.53
A730009E18Rik	AK047818	2.09	4.35
Abcc2	NM_013806	2.09	2.06
Abcc4	NM_001033336	10.57	8.29
Abcc5	NM_013790	2.32	4.59
Abhd2	NM_018811	4.96	2.36
Acnat2	NM_145368	5.50	3.19
Acsm2	NM_146197	6.38	3.91
Adam32	NM_153397	7.36	6.91
Adam8	NM_007403	2.72	3.38
Aebp2	NM_001005605	2.39	2.05
Aen	NM_026531	4.07	3.24
Afp	NM_007423	12.08	8.91
Airn	AK032756	4.03	4.26
Akap2	NM_001035533	2.29	2.26
Akr1c18	NM_134066	13.96	2.49
Akr1c19	NM_001013785	2.73	2.56
Aldh1a1	NM_013467	2.54	2.78
Aldh1b1	NM_028270	2.71	2.10
Amz1	NM_173405	2.38	4.47
Ankrd56	NM_175270	4.71	3.62
Aplp1	NM_007467	2.51	2.51
Apoa4	NM_007468	2.47	2.10
Arhgap12	NM_001039692	2.34	2.49
Arntl	NM_007489	12.61	4.14
Atf3	NM_007498	4.42	2.84
Atp6v0e2	NM_133764	5.49	2.11

Atpif1	NM_007512	4.45	2.83
Aurka	NM_011497	2.75	2.56
Axin2	NM_015732	3.54	2.75
B930041F14Rik	NM_178699	4.45	4.33
BC049762	NM_177567	2.82	3.27
Bcor	NM_029510	3.70	2.66
Btg3	NM_009770	5.60	3.54
C030034I22Rik	NR_026848	2.12	2.40
Car15	NM_030558	2.94	3.34
Car2	NM_009801	16.98	12.98
Cbr1	NM_007620	3.39	3.23
Cbr3	NM_173047	11.18	20.51
Ccdc93	NM_001025156	2.48	2.09
Ccl2	NM_011333	3.62	6.33
Ccng1	NM_009831	4.15	2.46
Ccr7	NM_007719	2.09	3.31
Cd36	NM_007643	4.90	3.79
Cd63	NM_001042580	7.73	5.18
Cd72	NM_001110320	2.10	2.62
Cd79b	NM_008339	2.56	2.96
Cda	NM_028176	5.58	3.49
Cdc20	NM_023223	8.97	4.16
Cdca3	NM_013538	5.30	2.84
Cdca5	NM_026410	3.46	2.20
Cdca8	NM_026560	2.40	2.23
Cdkn1a	NM_007669	18.92	11.79
Cenpt	NM_177150	2.40	2.26
Cgref1	NM_026770	2.36	3.61
Clec7a	NM_020008	2.58	4.37
Cnksr3	NM_172546	2.55	2.12
Col7a1	NM_007738	5.64	4.35
Crym	NM_016669	3.41	2.35
Csnk1g1	NM_173185	2.24	2.09
Ctps	NM_016748	2.13	3.25
Cxcl10	NM_021274	6.06	7.85
Cyp1a1	NM_009992	3.24	4.94
Cyp2a21-ps	XM_286199	6.78	5.95
Cyp2a4	NM_009997	9.46	6.04
Cyp4a14	NM_007822	22.08	4.69

D230034L24Rik	AK084380	3.42	4.21
D5Ertd579e	XM_001474408	2.52	2.51
D830044D21Rik	AK077973	5.51	2.22
Dcaf4	NM_030246	2.46	2.16
Dnmt3b	NM_001003961	3.76	2.62
Dusp6	NM_026268	2.70	3.20
Dyrk3	NM_145508	3.03	2.45
EG634650	NM_001039647	3.26	4.31
Egr1	NM_007913	4.50	2.75
ENSMUST00000021323	ENSMUST00000021323	2.01	2.79
ENSMUST00000063955	ENSMUST00000063955	2.59	4.39
ENSMUST00000085290	ENSMUST00000085290	2.02	2.14
ENSMUST00000100512	ENSMUST00000100512	2.65	3.71
ENSMUST00000102977	ENSMUST00000102977	4.31	3.19
ENSMUST00000108263	ENSMUST00000108263	2.09	2.24
Entpd5	NM_001026214	2.03	2.16
Ephx1	NM_010145	2.32	2.16
Evi2a	NM_001033711	2.23	3.48
Evpl	NM_025276	7.05	3.99
Fam189b	NM_001014995	2.01	2.09
Fam89a	NM_001081120	3.89	2.95
Fst	NM_008046	2.98	3.58
Fth1	NM_010239	2.45	2.35
Gbp3	NM_018734	2.24	3.74
Gclc	NM_010295	3.85	3.36
Gm10030	XM_001472570	2.75	4.85
Gm10639	NM_001122660	17.31	15.30
Gm3367	XM_001476471	2.18	2.15
Gm379	XM_142052	4.77	2.28
Gm5678	XM_487442	3.35	3.22
Gm6135	XM_895691	11.92	2.84
Gm7231	XM_001477336	2.95	2.78
Gm9454	XM_001477565	4.67	7.30
Golm1	NM_027307	3.04	3.15
Grhl1	NM_145890	2.11	2.29
Gsta1	NM_008181	21.32	22.67
Gsta2	NM_008182	10.19	7.87
Gstm1	NM_010358	2.84	3.27
Gstm2	NM_008183	2.66	2.43

Gstm3	NM_010359	4.32	3.84
Gstm4	NM_026764	2.11	2.06
H2afj	NM_177688	2.45	2.02
Hist1h1c	NM_015786	4.75	2.71
Hs3st6	NM_001012402	2.92	2.20
Hsd3b4	NM_001111336	10.91	2.13
Hunk	NM_015755	2.80	2.48
Icam1	NM_010493	2.04	2.27
Id1	NM_010495	7.20	2.03
Id2	NM_010496	3.46	4.93
Ifrd1	NM_013562	2.57	2.46
Ikbkg	NM_010547	3.00	2.91
Il4i1	NM_010215	2.89	2.33
Incenp	NM_016692	3.19	2.82
Isyna1	NM_023627	3.20	2.82
Itga4	NM_010576	2.43	4.69
Itgax	NM_021334	2.72	2.33
Jub	NM_010590	3.87	3.89
Kif22	NM_145588	3.18	3.12
Kif5a	NM_001039000	4.05	2.24
Klhl25	NM_182782	3.51	2.51
Krt31	NM_010659	3.01	3.29
Ldhb	NM_008492	3.30	2.10
Lgals1	NM_008495	2.60	2.79
Lnx1	NM_001159577	2.67	3.09
LOC100044531	XM_001472661	2.08	2.20
LOC100045552	XM_001474520	2.44	2.43
LOC100047597	XM_001478475	2.46	2.20
LOC625953	XM_001480391	13.77	14.60
Lonrf3	NM_028894	5.64	4.01
Lrrc51	NM_001162974	3.34	2.47
Ly6c1	NM_010741	4.98	2.33
Ly6d	NM_010742	15.83	15.60
Lzic	NM_026963	3.76	2.56
Mad2l1	NM_019499	2.93	2.14
Mest	NM_008590	3.02	2.42
Mki67	NM_001081117	6.27	2.82
Mpa2l	NM_194336	2.14	4.96
Mpzl1	NM_001001880	4.67	2.35

Myc	NM_010849	2.04	2.17
Neil2	NM_201610	3.53	2.84
Nfe2l2	NM_010902	2.54	3.62
Nipa1	NM_153578	3.95	2.14
Nqo1	NM_008706	8.20	2.92
Nrg1	NM_178591	7.82	5.24
Nrxn2	NM_020253	2.34	3.09
Nt5dc2	NM_027289	2.79	2.29
Nt5e	NM_011851	11.56	2.17
Ntrk2	NM_001025074	3.13	2.76
Omp	NM_011010	2.59	2.49
Osgin1	NM_027950	2.69	5.73
Ovgp1	NM_007696	4.41	6.79
Pbld	NM_026701	2.17	2.18
Pcp4l1	NM_025557	6.58	3.62
Pdgfa	NM_008808	2.10	2.02
Pdk4	NM_013743	7.53	5.69
Pfkfb4	NM_173019	2.62	2.38
Phlda3	NM_013750	15.15	6.84
Pik3r3	NM_181585	2.12	2.20
Pitpnm1	NM_001136078	2.04	2.48
Pkmyt1	NM_023058	2.53	2.22
Plk2	NM_152804	3.30	5.09
Pmvk	NM_026784	2.04	2.05
Ppfia4	NM_001144855	2.26	2.26
Ppfibp2	NM_008905	2.46	2.73
Prkab2	NM_182997	2.31	2.40
Prss8	NM_133351	4.98	4.03
Pvt1	NR_003368	3.34	3.92
Rab11fip5	NM_001003955	3.26	2.27
Rab34	NM_033475	2.13	2.01
Racgap1	NM_012025	3.65	2.34
Raet1e	NM_198193	2.57	3.06
Rasl11b	NM_026878	2.52	2.07
Rnd2	NM_009708	2.26	2.63
Robo1	NM_019413	3.55	2.04
Samd4	NM_001037221	3.63	2.58
Sccpdh	NM_178653	2.99	2.06
Scd2	NM_009128	16.96	5.31

Scgb1c1	NM_001099742	5.42	2.91
Sebox	NM_008759	3.32	2.48
Slc17a1	NM_009198	2.18	2.24
Slc1a5	NM_009201	4.55	2.85
Slc27a3	NM_011988	2.02	2.03
Slc48a1	NM_026353	2.13	2.14
Slpi	NM_011414	10.06	7.11
Smad7	NM_001042660	2.12	2.47
Smoc2	NM_022315	2.07	2.47
Srxn1	NM_029688	2.75	2.22
Tgm1	NM_019984	4.39	2.16
Tmem43	NM_028766	2.87	2.23
Tnfrsf10b	NM_020275	11.08	4.07
Tnfrsf12a	NM_013749	2.56	2.00
Tpm1	NM_001164248	3.23	2.67
Trdmt1	NM_010067	3.68	2.07
Trem2	NM_031254	4.87	2.85
Trip10	NM_134125	3.10	2.12
Trip13	NM_027182	3.34	3.05
Tuba8	NM_017379	16.37	4.46
Tubb2a	NM_009450	4.31	2.99
Ugt2b34	NM_153598	2.23	2.04
Vps37d	NM_177574	2.84	2.15
Wfdc15b	NM_138685	5.31	2.44
Xpo4	NM_020506	2.13	2.07
Zdhhc2	ENSMUST00000049389	2.20	2.01
Zfp7	NM_145916	2.70	2.19
Zmat3	NM_009517	3.89	3.00

Supplementary Table 7. Genes annotated in KEGG pathway database among those upregulated by TAA in both WT and AID Tg mice

Category	Gene					
Tumor suppressor genes	Atf3	Axin2	Btg3	Cdkn1a	Cxcl10	Dusp6
	Egr1	Id2	Mad2l1	Nfe2l2	Nqo1	Nrg1
	Plk2	Robo1	Tnfrsf10b	Tpm1		
Carcinogen-metabolic genes	Cbr1	Gsta1	Gsta2	Gstm1	Gstm2	Gstm3
	Gstm4	Ugt2b34				
Others	Abcc2	Abcc4	Abcc5	Acsm2	Afp	Akr1c18
	Aldh1a1	Aldh1b1	Apoa4	Arntl	Atp6v0e2	Aurka
	Car15	Car2	Cbr3	Ccl2	Ccng1	Ccr7
	Cd36	Cd63	Cd72	Cd79b	Cda	Cdc20
	Cdca5	Clec7a	Col7a1	Csnk1g1	Ctps	Cyp1a1
	Cyp2a4	Cyp4a14	Dnmt3b	Entpd5	Ephx1	Fst
	Fth1	Gclc	H2afj	Hsd3b4	Icam1	Id1
	Ikbkg	Il4i1	Isyna1	Itga4	Itgax	Kif5a
	Ldhb	Mpzl1	Myc	Neil2	Nrxn2	Nt5e
	Ntrk2	Pdgfa	Pfkfb4	Pik3r3	Pkmyt1	Pmvk
	Ppfia4	Prkab2	Rab11fip5	Raet1e	Scd2	Slc1a5
	Smad7	Tnfrsf12a	Trem2	Trip10	Tuba8	Tubb2a
	Vps37d	Zmat3				

Supplementary Table 8. List of somatic mutations detected by deep sequencing.

Sample index	Strain	TAA	Mouse	T or NT*	Gene	mRNA position	Nucleotide change	Mutant allele frequency (%)	Amino acid change	Functional predictions by SIFT	Common mutations between T and NT*
1	AID Tg	(+)	#1	NT	Dusp6	519	G>A	1.37	NS	To	0
1	AID Tg	(+)	#1	NT	Dusp6	647	G>A	1.77	NS	D	1
1	AID Tg	(+)	#1	NT	Dusp6	667	G>A	9.45	NS	D	0
1	AID Tg	(+)	#1	NT	Dusp6	727	G>A	2.22	NS	To	1
1	AID Tg	(+)	#1	NT	Dusp6	749	G>A	3.69	S	To	1
1	AID Tg	(+)	#1	NT	Dusp6	902	C>T	1.61	S	To	0
1	AID Tg	(+)	#1	NT	Egr1	433	G>A	21.82	NS	D	1
1	AID Tg	(+)	#1	NT	Egr1	455	G>A	20.91	NS	D	0
1	AID Tg	(+)	#1	NT	Egr1	503	G>A	18.18	NS	D	0
1	AID Tg	(+)	#1	NT	Egr1	522	C>T	21.82	S	To	0
1	AID Tg	(+)	#1	NT	Egr1	701	C>T	1.08	NS	D	0
1	AID Tg	(+)	#1	NT	Egr1	1076	G>A	2.04	NS	D	0
1	AID Tg	(+)	#1	NT	Egr1	1175	G>A	1.1	NS	D	0
1	AID Tg	(+)	#1	NT	Id2	138	G>A	2.62	NS	To	1
1	AID Tg	(+)	#1	NT	Id2	346	G>A	3.23	S	To	0
2	AID Tg	(+)	#1	T1	Dusp6	554	C>T	27.19	S	To	0
2	AID Tg	(+)	#1	T1	Dusp6	647	G>A	68.43	NS	D	1
2	AID Tg	(+)	#1	T1	Dusp6	715	G>A	39.86	NS	D	0
2	AID Tg	(+)	#1	T1	Dusp6	736	C>A	40.04	NS	To	0
2	AID Tg	(+)	#1	T1	Egr1	418	C>A	21.4	NS	To	0
2	AID Tg	(+)	#1	T1	Egr1	433	G>A	20.99	NS	D	1
2	AID Tg	(+)	#1	T1	Egr1	917	C>T	32.81	NS	D	0
2	AID Tg	(+)	#1	T1	Egr1	1001	C>T	2.08	NS	To	0
2	AID Tg	(+)	#1	T1	Id2	165	C>T	1.68	NS	D	0
2	AID Tg	(+)	#1	T1	Id2	277	G>A	27.75	S	To	0
2	AID Tg	(+)	#1	T1	Id2	307	G>A	36.65	S	To	0
3	AID Tg	(+)	#1	T2	Dusp6	540	C>T	3.04	S	To	0
3	AID Tg	(+)	#1	T2	Dusp6	545	G>A	2.66	S	To	0
3	AID Tg	(+)	#1	T2	Dusp6	647	G>T	1.04	NS	D	1

3	AID Tg	(+)	#1	T2	Dusp6	693	A>G	2.34	NS	To	0
3	AID Tg	(+)	#1	T2	Dusp6	715	G>A	1.56	NS	D	0
3	AID Tg	(+)	#1	T2	Dusp6	726	C>T	1.3	NS	To	0
3	AID Tg	(+)	#1	T2	Dusp6	727	G>A	5.71	NS	To	1
3	AID Tg	(+)	#1	T2	Dusp6	730	G>T	2.34	NS	To	0
3	AID Tg	(+)	#1	T2	Dusp6	749	G>A	1.82	S	To	1
3	AID Tg	(+)	#1	T2	Dusp6	887	G>T	5.11	NS	To	0
3	AID Tg	(+)	#1	T2	Egr1	433	G>A	67.69	NS	D	1
3	AID Tg	(+)	#1	T2	Egr1	1156	G>A	57.3	NS	D	0
3	AID Tg	(+)	#1	T2	Id2	138	G>A	27.6	NS	To	1
4	AID Tg	(+)	#2	NT	Dusp6	545	G>A	1.19	S	To	1
4	AID Tg	(+)	#2	NT	Dusp6	546	C>T	1.43	S	To	0
4	AID Tg	(+)	#2	NT	Dusp6	667	G>A	1.15	NS	D	1
4	AID Tg	(+)	#2	NT	Dusp6	727	G>A	2.42	NS	To	1
4	AID Tg	(+)	#2	NT	Dusp6	728	C>T	1.27	S	To	0
4	AID Tg	(+)	#2	NT	Dusp6	749	G>A	2.42	S	To	1
4	AID Tg	(+)	#2	NT	Egr1	407	G>A	7.69	NS	To	0
4	AID Tg	(+)	#2	NT	Egr1	434	C>T	3.85	NS	D	0
4	AID Tg	(+)	#2	NT	Egr1	461	G>A	9.62	NS	To	1
4	AID Tg	(+)	#2	NT	Egr1	476	G>A	9.62	NS	D	0
4	AID Tg	(+)	#2	NT	Egr1	509	G>A	3.85	NS	To	0
4	AID Tg	(+)	#2	NT	Egr1	521	G>A	3.85	NS	To	0
4	AID Tg	(+)	#2	NT	Egr1	1113	C>T	3.34	S	To	0
4	AID Tg	(+)	#2	NT	Id2	138	G>A	2.48	NS	To	1
4	AID Tg	(+)	#2	NT	Id2	280	G>A	1.69	S	To	1
5	AID Tg	(+)	#2	T	Dusp6	545	G>A	2.29	S	To	1
5	AID Tg	(+)	#2	T	Dusp6	648	C>T	3.14	S	To	0
5	AID Tg	(+)	#2	T	Dusp6	667	G>A	1.89	NS	D	1
5	AID Tg	(+)	#2	T	Dusp6	716	C>T	1.05	S	To	0
5	AID Tg	(+)	#2	T	Dusp6	727	G>A	7.76	NS	To	1
5	AID Tg	(+)	#2	T	Dusp6	749	G>A	3.35	S	To	1
5	AID Tg	(+)	#2	T	Dusp6	752	G>A	1.68	S	To	0
5	AID Tg	(+)	#2	T	Egr1	461	G>A/T	5.2/1.16	NS	To	1
5	AID Tg	(+)	#2	T	Egr1	513	C>T	5.2	S	To	0
5	AID Tg	(+)	#2	T	Egr1	657	G>A	1.02	S	To	0

5	AID Tg	(+)	#2	T	Id2	138	G>A	2.48	NS	To	1
5	AID Tg	(+)	#2	T	Id2	187	G>A	1.24	S	To	0
5	AID Tg	(+)	#2	T	Id2	278	C>T	3.68	NS	NO	0
5	AID Tg	(+)	#2	T	Id2	280	G>A	2.45	S	To	1
6	AID Tg	(+)	#3	NT	Dusp6	511	G>A	1.28	NS	To	0
6	AID Tg	(+)	#3	NT	Dusp6	519	G>A	1.53	NS	To	0
6	AID Tg	(+)	#3	NT	Dusp6	545	G>A	1.02	S	To	0
6	AID Tg	(+)	#3	NT	Dusp6	546	C>T	2.3	S	To	0
6	AID Tg	(+)	#3	NT	Dusp6	567	C>T	1.79	S	To	0
6	AID Tg	(+)	#3	NT	Dusp6	648	C>T	2.86	S	To	0
6	AID Tg	(+)	#3	NT	Dusp6	659	G>A	1.15	S	To	0
6	AID Tg	(+)	#3	NT	Dusp6	667	G>A	1.72	NS	D	0
6	AID Tg	(+)	#3	NT	Dusp6	671	C>T	3.44	S	To	0
6	AID Tg	(+)	#3	NT	Dusp6	672	C>T	5.73	S	To	0
6	AID Tg	(+)	#3	NT	Dusp6	687	C>T	1.53	NS	D	0
6	AID Tg	(+)	#3	NT	Dusp6	727	G>A	14.5	NS	To	0
6	AID Tg	(+)	#3	NT	Dusp6	747	G>A	2.1	NS	D	0
6	AID Tg	(+)	#3	NT	Dusp6	749	G>A	5.15	S	To	0
6	AID Tg	(+)	#3	NT	Dusp6	912	C>T	2.11	S	To	0
6	AID Tg	(+)	#3	NT	Dusp6	929	C>T	2.42	S	To	0
6	AID Tg	(+)	#3	NT	Dusp6	931	G>A	1.51	NS	To	0
6	AID Tg	(+)	#3	NT	Egr1	407	G>A	6.48	NS	To	0
6	AID Tg	(+)	#3	NT	Egr1	431	G>A	3.7	NS	D	0
6	AID Tg	(+)	#3	NT	Egr1	468	C>T	9.26	S	To	0
6	AID Tg	(+)	#3	NT	Egr1	654	G>A	1.02	S	To	0
6	AID Tg	(+)	#3	NT	Id2	138	G>A	2.07	NS	To	0
7**	AID Tg	(+)	#3	T	-	-	-	-	-	-	-
8	AID Tg	(-)	#4	NT	Dusp6	648	C>T	1.08	S	To	0
8	AID Tg	(-)	#4	NT	Egr1	407	G>A	1.26	NS	To	0
8	AID Tg	(-)	#4	NT	Id2	343	C>T	1.81	S	To	0
9	AID Tg	(-)	#5	NT	Id2	139	C>T	1.17	S	To	0
10**	WT	(+)	#6	NT	-	-	-	-	-	-	-
11**	WT	(-)	#7	NT	-	-	-	-	-	-	-

T, tumor; NT, nontumor; NS, nonsynonymous mutation; S, synonymous mutation; SIFT, Sorting Intolerant From Tolerant; To, tolerated; D, damaging; NO, nonsense mutation.

* T1 and T2 are distinct tumors which developed in the #3 mouse.

** These samples have no somatic mutations in the analyzed genes.